1 **Planktonic foraminifera assemblage composition and flux dynamics inferred from an annual**
2 **sediment trap record in the Central Mediterranean Sea**
3
4 Thibauld M. Béjard[1*], Andrés S. Rigual-Hernández[1], Javier Pérez Tarruella[1], José-Abel Flores[1], Anna
5 Sanchez-Vidal[2], Irene Llamas-Cano[2], Francisco J. Sierro[1]
6
7 1. Área de Paleontología, Departamento de Geología, Universidad de Salamanca, Salamanca, Spain
8 2. GRC Geociències Marines, Departament de Dinàmica de la Terra i de l'Oceà, Universitat de
9 Barcelona, Spain
10
11 *** Correspondence:** Thibauld M. Béjard (thibauld.bejard@usal.es)
12
15
16 **Abstract**
17
18 The Sicily Channel, located in the Central Mediterranean Sea, represents a key point for the regional
19 oceanographic circulation as it is considered the sill that separates the western and eastern basins.
20 Therefore, it is considered a unique zone regarding the well-documented west-to-east
21 Mediterranean productivity gradient. Here we present a time series of settling planktonic
22 foraminifera assemblages from November 2013 to October 2014. 19 samples from the sediment
23 trap C01 deployed at a water depth of around 400 m have been used. More than 3700 individuals
24 and 15 different species have been identified. *Globorotalia inflata*, *Globorotalia truncatulinoides*,
25 *Globigerina bulloides*, *Globigerinoides ruber* and *ruber* (pink) were the five main species identified,
26 accounting for more than 85% of the total foraminifera.
27 The total planktonic foraminifera flux mean value was 630 shells m^{-2} d^{-1}, with a minimum value of
28 45 shells m^{-2} d^{-1} displayed during late autumn 2013 and a maximum of 1890 shells m^{-2} d^{-1} reached
29 during spring 2014. This is likely due to the regional oceanographic configuration and the marked
30 seasonality in the surface circulation. During spring and winter, the Atlantic waters dominate the
31 surface circulation, bringing cool and nutrient enriched waters. This results in a planktonic
32 foraminifera flux increase and a dominance of western basin taxa. During summer and autumn, the
33 circulation is dominated by the eastern warm and oligotrophic Levantine water, which leads to a
34 planktonic foraminifera flux decrease and the dominance of easter basin species. Our comparison
35 with satellite derived SST and chlorophyll-*a* data showed that *G. inflata* was associated with cool
36 and nutrient rich conditions, while both *G. ruber* morphotypes were associated with warm and
37 oligotrophic conditions. However, no trends were identified for *G. truncatulinoides* or *G. bulloides*.
38 As the latter species flux increased coincidently with that of benthic foraminifera one, we considered
39 that this species might have a resuspended origin.
40 The comparison of the Sicily Channel data with other Mediterranean time series indicates that the
41 annualized planktonic foraminifera flux was lower than in the westernmost Alboran Sea but higher
42 than in the easternmost Levantine basin. The Sicily Channel species diversity was the highest among

43 the compared zones, highlighting the influence of the different basins and its transitional aspect
44 from a planktonic foraminifera population perspective.
45 Finally, we compared the settling planktonic foraminifera assemblage with the assemblages from
46 seabed sediment located in the vicinity of the Sicily Channel. The differences with the seabed
47 populations varied according to the sites studied. The deep-dwelling species dominated the settling
48 assemblages samples, while eutrophic and oligotrophic species were more abundant in the
49 sediment. Finally, a high-resolution chronology comparison allowed to show that this planktonic
50 foraminifera population shift likely developed during the late Holocene prior to the industrial period,
51 however, its causes remain uncertain.
52
53 **1. Introduction**
54
55 Planktonic foraminifera are a group of marine calcareous single-celled protozoans with a
56 cosmopolitan distribution. Around 50 morphospecies of planktonic foraminifera have been
57 described in today's oceans (Schiebel and Hemleben, 2017), and although most of those species are
58 surface dwellers, some species can be found in waters below 2000 m (Schiebel and Hemleben,
59 2005). Their abundance and distribution are affected by a wide array of factors, such as
60 temperature, salinity, chlorophyll-*a* and nutrient concentrations, among others (Hemleben et al.,
61 1989; Schiebel and Hemleben, 2005). According to Schiebel, (2002), the production and export of
62 their calcareous shells account for 23 to 56% of the open marine $CaCO_3$ flux, thereby playing a key
63 role in the marine carbon cycle. Moreover, the high preservation potential of their shells makes
64 them one of the most used groups for multi-proxy studies. Numerous paleoclimatic (e.g. Barker and
65 Elderfield, 2002; Lirer et al., 2014; Margaritelli et al., 2020; Sierro et al., 2005) and
66 paleoceanographic (Cisneros et al., 2016; Ducassou et al., 2018; Margaritelli et al., 2022; Toucanne
67 et al., 2007) reconstructions have used planktonic foraminifera as a proxy. In addition, their capacity
68 to reflect the water column's chemical properties has propelled studies that have focused on the
69 impact of recent climate and environmental variability on the water column in different parts of the
70 ocean (e.g. Azibeiro et al., 2023; Beer et al., 2010; Bijma et al., 2002; Chapman, 2010; Marshall et
71 al., 2013; Osborne et al., 2016). As marine calcifying organisms, they are considered particularly
72 vulnerable to the ongoing ocean warming and acidification (Bijma et al., 2002; Fox et al., 2020). Shell
73 calcification of several foraminifera species has been showed to decrease in response to ocean
74 acidification, and therefore, changes in the weight of their shells are considered an indicator of the
75 ocean acidification impact on different timescales (Béjard et al., 2023; de Moel et al., 2009; Fox et
76 al., 2020; Kroeker et al., 2013; Moy et al., 2009; Pallacks et al., 2023). In contrast, ocean warming
77 has been proposed to produce an opposite effect on foraminifera calcification, as some studies have
78 documented that an increase in water temperature results in larger shells and enhanced growth
79 rates (Lombard et al., 2011, 2009; Schmidt et al., 2006).
80 Despite the wide array of studies focused on planktonic foraminifera ecology and distribution,
81 several aspects of their ecology remain uncertain, such as their ecological tolerance limits (Mallo et
82 al., 2017), their geographical and temporal distributions and contribution to the marine
83 biogeochemical cycles (Jonkers and Kučera, 2015). As major contributors to the pelagic calcite
84 production (Schiebel, 2002), understanding their life cycle on different time scales is essential for

constraining the role they play in the marine carbon cycle and the impact of environmental change on these organisms. In this regard, sediment traps represent a powerful tool to improve our knowledge of planktonic foraminifera ecology and their impact on the biogeochemical cycles, as they allow the monitoring of foraminifera shell fluxes for extended periods, thereby allowing to document their seasonal and interannual variability and estimate their contribution to annual budgets of carbonate export to the seafloor (Jonkers et al., 2019).

The Mediterranean Sea is a semi-enclosed sea often considered a "miniature ocean" (Bethoux et al., 1999) from an oceanographic point of view or a "laboratory basin" (Bergamasco and Malanotte-Rizzoli, 2010) for studying processes occurring on a global scale. In addition, it is supersaturated regarding calcite (Álvarez et al., 2014), a key aspect in foraminifera studies, as this parameter favors shell preservation and represents one of the main environmental controls on planktonic foraminifera abundance and calcification (Aldridge et al., 2012; Marshall et al., 2013; Osborne et al., 2016). These features make it an interesting zone of the global ocean to study the life cycle and seasonal response to changing environmental conditions of calcifying plankton. The Sicily Channel, in the central Mediterranean, is the sill that divides the Mediterranean into its western and eastern basins. It is a choke point for the regional surface and deep-water circulation (Malanotte-Rizzoli et al., 2014; Pinardi et al., 2015) and a transition region regarding the well-known west-to-east oligotrophy gradient, functioning as a "biological corridor" (Siokou-Frangou et al., 2010) known in the Mediterranean (Navarro et al., 2017).

Despite these characteristics, time series that focused on planktonic foraminifera in the Mediterranean Sea are scarce. So far, the best monitored regions are the Alboran Sea (Bárcena et al., 2004; Hernández-Almeida et al., 2011), the Gulf of Lions (Rigual-Hernández et al., 2012), and more recently, the Levantine Basin (Avnaim-Katav et al., 2020). The latter studies showed that planktonic foraminifera followed a unimodal distribution with maximum shell export occurring during the months of April-May, February-March and February respectively, which agreed with the local hydrographic conditions. However, the central Mediterranean remains understudied and poorly documented regarding both continuous time series and planktonic foraminifera dynamics.
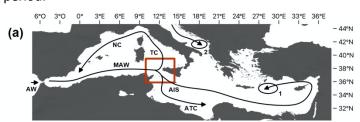
Therefore, this work aims to provide new planktonic foraminifera data from a sediment trap mooring line located in the Channel of Sicily to improve the current knowledge about their community composition and seasonal patterns in the central Mediterranean. For that purpose, here we document the magnitude and composition of planktonic foraminifera fluxes identified in the >150 μm fraction (i.e. the most commonly used size fraction for studying planktonic foraminifera distribution) from November 2013 to October 2014. We compare our planktonic foraminifera data with a suite of environmental parameters to assess the main environmental drivers that control the seasonal variations in the composition and abundance of the sinking planktonic foraminifera assemblages. To provide further insight on a regional and global scale of the planktonic foraminifera association and fluxes identified here, we compare our data with other time series from the Mediterranean, Atlantic Ocean and other regions of the world's oceans. Lastly, we compared the assemblages collected by the sediment with seabed sediment located in the vicinity of the Sicily Channel to document the potential shift in recent planktonic foraminifera populations.
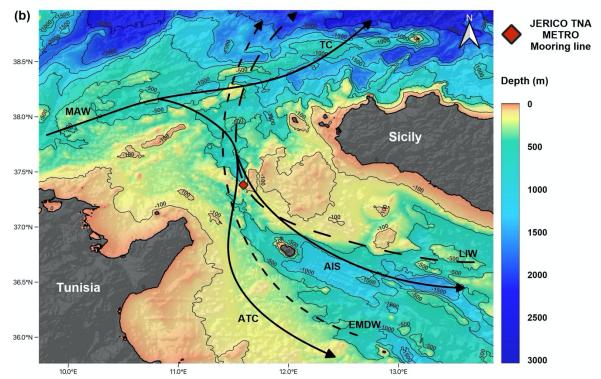
2. Study area

The Mediterranean is an elongated, semi-enclosed sea with an anti-estuarine circulation. It is considered to be a concentration basin (Bethoux et al., 1999) in which the evaporation exceeds the freshwater inputs, forcing a negative hydrological balance (Robinson and Golnaraghi, 1994). This negative balance is compensated by the entrance of surface oceanic water from the Atlantic Ocean through the Channel of Gibraltar. The colder and nutrient richer Atlantic Waters (AW) spread eastward into the Mediterranean basin (Millot, 1991; Pinardi et al., 2015), where they progressively become warmer, saltier and more oligotrophic as they mix with resident waters (Modified Atlantic Waters – MAW. Also known as Atlantic Waters – AW). MAW circulate following a cyclonic circuit along the Algerian coast (Algerian Current – AC) (Malanotte-Rizzoli et al., 2014; Millot, 1999) and divide into two main branches at the entrance of the Sicily Channel (Figure 1a). One of these branches spreads into the northwestern part of the basin, into the Tyrrhenian Sea, where it continues its path cyclonically. The second branch flows south of Sicily into the Ionian Sea (Lermusiaux and Robinson, 2001). In the Sicily channel itself, the water masses are split again in two different streams (Béranger et al., 2004): (i) the Atlantic Tunisian Current (ATC) that flows to the southeast following the African coast; and (ii) the Atlantic Ionian Stream (AIS) that flows into the deep eastern part of the basin (Figure 1b) and contributes to the MAW transport in the eastern Mediterranean (Jouini et al., 2016; Lermusiaux and Robinson, 2001).

The Sicily Channel is located in the central Mediterranean (Figure 1a) and acts as a sill that topographically separates the western and eastern Mediterranean basins. The circulation through the Sicily Channel is characterized by water masses that flow in opposite directions at different depths of the water column (Béranger et al., 2004; Garcia-Solsona et al., 2020; Pinardi et al., 2015; Schroeder et al., 2017). The Levantine Intermediate Water (LIW), which enters the Channel from the Ionian Sea, occupies the deeper part of the water column along with occasional thin Eastern Mediterranean Deep Water layers (Gasparini et al., 2005; Lermusiaux and Robinson, 2001). The Ionian Water (IW) can be present at intermediate depths (Figure 1), while the MAW cover the surface to subsurface part of the water column (Garcia-Solsona et al., 2020; Warn-Varnas et al., 1999). Temperature and salinity range from 15-17 °C and 37.2-37.8 psu for the MAW, 15-16.5 °C and 37.8-38.4 psu for the IW and 13.7-13.9°C and 38.7-38.8 psu for the LIW (Astraldi et al., 2002; Bouzinac et al., 1999; Robinson et al., 1999). Lastly, it is important to note, that the surface circulation in the Sicily Channel presents a large seasonal variability concerning the water masses distribution (Béranger et al., 2004; Lermusiaux and Robinson, 2001). Surface circulation experiences a substantial seasonality in the Sicily Channel: during late autumn to late spring, the MAW dominate the surface circulation, allowing nutrient and chlorophyll-enriched waters to enter the Channel (Astraldi et al., 2002; D'Ortenzio, 2009). In turn, summer and autumn are dominated by LIW waters. Deep-water circulation remains relatively stable on a seasonal scale (Béranger et al., 2004) with a continuous LIW presence over the year. Finally, during summer, an upwelling settles in the Sicily Channel, allowing the impoverished LIW to reach the surface (Lermusiaux and Robinson, 2001).

Regarding its nutrient distributions, the Mediterranean Sea is generally considered an oligotrophic to ultraoligotrophic sea (Krom et al., 1991). However, this oligotrophy is not homogenous and displays a clear west-to-east gradient which is reflected in the nutrient concentration and algal

4

167 biomass accumulation derived from colour remote sensing (Navarro et al., 2017; Siokou-Frangou et
168 al., 2010). The eastern part of the Mediterranean is considered to be more nutrient depleted than
169 the western part of the basin (Krom et al., 2005; Raimbault et al., 1999), with N:P ratios around 50:1
170 (Krom et al., 2005). At times of maximum annual algal concentration, primary productivity (PP) in
171 the Levantine Basin reaches values of ca. 0.1 g C m^{-2}d^{-1} (Hazan et al., 2018). This value is substantially
172 lower than those recorded in the high productivity regions of the western basin such as the Gulf of
173 Lions, ca. 0.4-0.65 g C m^{-2}d^{-1} (Gaudy et al., 2003; Rigual-Hernández et al., 2012), or the Alboran Sea,
174 ca. 0.3-1.3 g C m^{-2}d^{-1} (Bárcena et al., 2004; Morán and Estrada, 2001) during the corresponding
175 period.

176
177 **Figure 1. (a)** Mediterranean Sea general surface circulation (Astraldi et al., 2002; Béranger et al., 2004;
178 Incarbona et al., 2011; Macias et al., 2019) and location of the study zone. The ellipses show the deep-
179 water formation zones for the LIW (1) and the EMDW (2). **(b)** Regional oceanographic and geographic
180 setting of the Sicily Channel. The red diamond represents the location of the JERICO TNA METRO C01
181 mooring line. Black continuous lines represent the surface circulation dominated by the Atlantic Ionian
182 Stream (AIS) and the Atlantic Tunisian Current (ATC); while dashed lines show deep-water circulation
183 influences by the Levantine Intermediate Water (LIW) and the Eastern Mediterranean Deep Water
184 (EMDW). The difference in the dashed lines period stands for the occasional aspect of the EMDW. The
185 topographic model was downloaded from the GEBCO database.

186

3. Material and methods

187

3.1. Field experiments

190

191 The sediment trap (Figure 1) was deployed in the C01 mooring line maintained by ISMAR-CNR in the
192 Sicily Channel (37.38°N, 11.59°E) thanks to a TransNational Access (TNA) call in the FP7 JERICO
193 project (Mediterranean sediment Trap Observatory). The mooring line was equipped with a
194 sequential sampling sediment trap located 413 m below the sea surface in a water column of around
195 450 m deep. The sediment trap was a PPS3/3 model, conical in shape with a 2.5 height/diameter
196 ratio and equipped with 12 sampling cups. Further information about this sediment trap
197 configuration and model can be found in Heussner et al., (2006, 1990).
198 Here we present data from November 2013 to mid-October 2014. The sampling period was 15 to
199 16 days from November 2013 to July 2014 and from September 2014 to October 2014. Between
200 July 2014 and September 2014, the sampling was set to 31 days. Before deployment and to limit the
201 degradation of the material caught, sediment trap sampling cups from both mooring lines were
202 filled with a 5% formalin solution prepared with 40% formaldehyde mixed with 0.45 μm filtered
203 seawater. The solution was then buffered with sodium borate to keep the pH stable and prevent
204 the dissolution of carbonate.

205

3.2 Processing of sediment trap samples

207

208 After the recovery, the cups were stored at 2-4°C until their processing according to the procedure
209 of Heussner et al., (1990). In the laboratory, the largest swimmers that entered the trap were
210 removed by wet sieving through a 1 mm nylon and samples were subsequently split into 6 aliquots
211 using a peristaltic pump. One sub-sample was used for total mass flux measurements, after having
212 <1mm swimmers and formaldehyde removed.
213 Another subsample of a total of 19 samples from the sediment trap were processed for
214 micropaleontological analyses in the micropaleontology laboratory of the Geology department at
215 the University of Salamanca. The samples consisted of aliquots of 1/6 of the original mooring line
216 cups and were preserved in seawater, with a pH between 7.6 and 7.8. All samples were first wet
217 sieved to separate the <63μm fraction and then dry sieved to separate the 63-150 and >150 μm
218 fractions. The washing was carried out with a potassium phosphate-buffered solution (pH= 7.5) to
219 prevent carbonate dissolution.

220

3.3 Planktonic foraminifera identification, flux calculations and imaging

222

223 The planktonic foraminifera identification (Plate 1) and counting to the species level were carried
224 out in the >150 μm fraction using a microscope (Leica Wild M3B). To have a representative picture
225 of the planktonic foraminifera population, the complete samples were analyzed (i.e. no splits were
226 applied). Identification was carried out according to Schiebel and Hemleben, (2017). A total of 15

species were identified (Plate 1): *Globigerinella siphonifera*, *G. calida*, *Globigerinoides sacculifer*, *G. ruber*, *G. ruber* (pink), *Globoturborotalita tenella*, *G. rubescens*, *Orbulina universa*, *Globorotalia truncatulinoides*, *G. inflata*, *G. scitula*, *Globigerina bulloides*, *G. falconensis*, *Neogloboquadrina incompta* and *Turborotalita quinqueloba* (Plate 1). In addition, benthic foraminifera shells were identified to the lowest taxonomic level possible and counted. The 150 μm size limit was used to compare our results with other time series and seabed sediment populations as it is widely used in planktonic foraminifera studies, however, we acknowledge that some "small-sized" species such as *N. incompta* and *G. tenella* may be undersampled as their adult size tends to be smaller (Chernihovsky et al., 2023).

The foraminifera fluxes were calculated according to the following formula:

$$PF \ (shells \ m^{-2} \ d^{-1}) = \frac{(N \ x \ aliq.) \ x \ SD^{-1}}{0.1256}$$

"PF" stands for planktonic foraminifera, "N" accounts for the number of individuals identified, "aliq." refers to the aliquot (1/6 for all samples) and "SD" represents the sampling interval that the sediment trap cup stayed open. Relative abundance for each species was also calculated for all samples.

Here we refer to the planktonic foraminifera collected by the sediment trap as the settling assemblage.

Lastly, to describe the seasonal flux variations and to put our results into a regional context and be coherent with previous studies, each season was defined as spring (March–May), summer (June–August), autumn (September–November) and winter (December–February).

To showcase the species collected by the traps (Plate 1), foraminifera imaging was carried out using a Nikon SMZ18 stereomicroscope equipped with a Nikon DS-Fi3 camera and the image processing software NISElements (version 5.11.03).

3.4. Satellite-derived environmental parameters

To assess the possible relationship of planktonic foraminifera fluxes with environmental variability, satellite-derived chlorophyll-*a* and Sea Surface Temperatures (SSTs) were retrieved from global data sets. Satellite-derived chlorophyll-*a* concentration (mg m^{-3}) was obtained from MODIS L3m satellite through NASA's Giovanni web interface with an 8-day and 4 km resolution for a 0.2 x 0.2° area around the mooring location between 01/10/2013 to 01/11/2014. Additionally, sea surface temperature SST (°C) were also obtained from the same site with the same resolution to use as a proxy for water temperature and water column stratification.

3.5 Planktonic foraminifera flux and surface sediment data from other Mediterranean settings

In order to put into context our observations with the regional variability of planktonic foraminifera communities in the Mediterranean Sea, modern planktonic foraminifera flux datasets were retrieved from different sites. Foraminifera fluxes of: (i) the Levantine basin (LevBas) were obtained from Avnaim-Katav et al., (2020); (ii) the Gulf of Lions (stations Planier - PLA, and Lacaze Duthiers -

268 LCD) from Rigual-Hernández et al., (2012); (iii) and the Alboran Sea (stations ALB 1F and ALB 5F)
269 from both Bárcena et al., (2004) and Hernández-Almeida et al., (2011). The foraminifera fluxes of
270 the Gulf of Lions and Alboran Sea concerned the >150 μm fraction, while the ones from the
271 Levantine basin represented the >125 μm fraction (Figure 7).
272 Core-top data from the ForCenS database (Siccha and Kucera, 2017) was used to compare the
273 planktonic foraminifera abundance patterns from the C01 mooring line with the seabed sediment.
274 Only seabed sediment located on a 2.5 degree difference in both latitude and longitude was selected
275 to compare our data with sites in the vicinity of the Sicily Channel. This corresponded to a total of
276 16 core-tops part of the MARGO database. The complete details of the latter can be found in the
277 Supplementary data.
278 Additionally, the planktonic foraminifera population data from two box-cores analyzed by Incarbona
279 et al., (2019) were also included: sites 342 (36.42°N, 13.55°E) and 407 (36.23°N, 14.27°E). These two
280 sites are located in the Sicily Channel and they provide a robust chronology (^{210}Pb) that allowed to
281 document abundance changes across the recent Holocene. The dating covered the years 1558 to
282 1994 CE. Here we compared the sediment trap from the C01 mooring line samples with the mean
283 relative abundance from the 23 (site 342) and 24 (site 407) samples available.
284 Finally, to have a more complete picture of the modern planktonic foraminifera communities
285 currently living the surface ocean, the annual integrated data of our sediment trap was compared
286 with the BONGO nets data from Mallo et al., (2017), specifically, with the sample retrieved in the
287 axis of the Sicily Channel (37.08°N, 13.18°E) in Spring 2013.
288
289 **3.6 Statistical analysis**
290
291 To have uninterrupted monthly and daily values from NASA's Giovanni environmental parameters
292 that coincide with the mean sampling date from the sediment trap, a daily resampling has been
293 carried out using QAnalySeries software.
294 Pearson correlation and *p*-value tests between the foraminifera abundances and the environmental
295 parameters (SST and chlorophyll-*a*) were carried out with the Past4 program. A $p < 0.05$ was used
296 to denote statistical significance.
297 In addition, a canonical correspondence analysis (CCA) was also used to evaluate the influence of
298 both SST and chlorophyll-*a* on foraminifera species fluxes. A CCA is a correspondence analysis of a
299 species matrix where each site has given values for one or more environmental variables (SST and
300 chlorophyll-*a* concentration in this case). The ordination axes are linear combinations of the
301 environmental variables. A CCA is considered an example of direct gradient analysis, where the
302 gradient in environmental variables is known and the species abundances/fluxes are considered to
303 be a response or to be affected by this gradient (Nielsen, 2000).
304 Additionally, to evaluate the magnitude of the foraminifera fluxes across major regions of the
305 Mediterranean, an estimation of the annual planktonic foraminifera flux (shells m^{-2} y^{-1}) was
306 calculated using the sediment trap data from the literature review and our study. To that purpose,
307 the data was annualized according to the following formula:
308 $$Annual\ PFF = \sum(PF\ x\ SD + cPF\ x\ mSD)$$

309 Where "PFF" stands for planktonic foraminifera flux (shells m^{-2} d^{-1}), "SD" accounts for sampling days,
310 "cPF" represents calculated planktonic foraminifera flux (shells m^{-2} d^{-1}) and "mSD" stands for missing
311 sampling days. "cPF" calculation depended on the site. For the datasets retrieved from the Sicily
312 Channel and the Levantine basin, less than 20 sampling days were missing, so the corresponding
313 planktonic foraminifera fluxes were replaced by the mean of the first and last flux values recorded.
314 The two datasets from the Alboran Sea displayed more than 70 missing days, so the corresponding
315 flux values used were a mean of the two closest months to the missing data. Concerning the two
316 time series from the Gulf of Lions, they covered more than one year. Therefore, a mean year was
317 estimated: a mean monthly flux value was calculated for all 12 months based on all the available
318 measurements and then multiplied by the corresponding mean duration of each month, and then,
319 all monthly fluxes were added together.
320 To compare the species richness and diversity across the previously described sites, Simpson (D) and
321 Shannon/Weiner (H/W) indexes were calculated. Here, we reported the inverse Simpson index (1-
322 D). None of these indexes were calculated for the Alboran Sea sites (ALB 1F and ALB 5F) because
323 only information about the four main species was documented (Bárcena et al., 2004; Hernández-
324 Almeida et al., 2011).
325 Finally, the squared chord distance (SCD) between the C01 sediment trap and every core top sample
326 downloaded from the ForCenS database (Siccha and Kucera, 2017) planktonic foraminifera relative
327 abundance was calculated. It is a widely used metric in palaeoecological and paleontological studies
328 as it is the most effective index for identifying the closest analogues in planktonic foraminifera
329 datasets (Prell, 1985). This is mainly because it shows the best balance in weighing the contribution
330 of abundant and rare species in a given association (Jonkers et al., 2019). In this study, SCD values
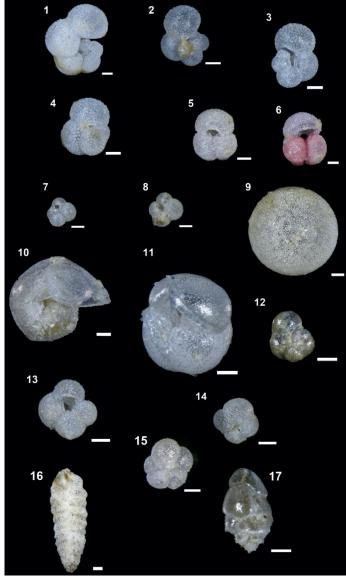331 lower than 0.25 have been considered as reliable analogues (Ortiz and Mix, 1997).
332

Plate 1. Planktonic **(1-15)** and the most common benthic foraminifera **(16-17)** species trapped in the sediment trap in mooring line C01. The white scale bars on all figures represent 100 μm. **(1)** *G. siphonifera,* side view. **(2)** *G. calida*, umbilical view. **(3)** *G. calida*, apertural view. **(4)** *G. sacculifer*, umbilical view. (**5**) *G. ruber*, umbilical view. **(6)** *G. ruber* (pink), umbilical view. **(7)** *G. tenella*, umbilical view. **(8)** *G. rubescens*, umbilical view. **(9)** *O. universa*. **(10)** *G. truncatulinoides*, umbilical view. **(11)**. *G. inflata*, apertural view. **(12)** *G. scitula*, umbilical view. **(13)** *G. bulloides*, umbilical view. **(14)** *N. incompta*, umbilical view. **(15)**. *T. quinqueloba*, umbilical view. **(16)** *Textularia spp.* **(17)** *Bulimina marginata*, apertural view.

4. Results

4.1 General considerations of the planktonic foraminifera assemblages

347 **Table 1.** Counts and key statistics of the planktonic foraminifera species and the benthic foraminifera
348 group from the > 150 μm fraction identified in the 19 sediment trap cups of the C01 mooring line. Mean,
349 maximum (Max), minimum (Min), standard deviation (SD) of the relative abundance and fluxes. Raw
350 counts also include a total and % of the total description. Note that *G. falconensis* was documented but
351 not included in the table due to its scarcity (only one individual was identified).

	G. sipho.	G. cal.	G. sacc.	G. rub.	G. rub.(p.)	G. ten.	G. rubesc.	O. univ.	G. truncat.	G. inf.	G. sci.	G. bull.	N. inc.	T. quin.	Benthics	Total planktonic
COUNTS (N)																
Mean	2.5	3.1	4.1	6.5	5.2	1.1	3.7	3.9	37.0	109.2	1.3	16.2	1.5	0.5	7.4	195.9
Max	6	11	10	22	40	5	9	15	118	456	7	111	8	3	42	633
Min	0	0	0	1	0	0	0	0	1	1	0	0	0	0	1	14
SD	1.8	2.8	3.2	5.6	9.2	1.5	2.5	4.1	33.2	132.5	2.3	26.4	2.3	1.1	9.2	
Total	48	59	78	124	99	21	71	74	703	2075	24	307	29	10	141	3723
% of total	1.3	1.6	2.1	3.3	2.7	0.6	1.9	2.0	18.9	55.7	0.6	8.2	0.8	0.3	3.3	
ABUNDANCES (%)																
Mean	2.0	2.7	2.8	5.5	5.7	0.9	4.0	3.0	20.5	41.6	1.9	7.3	1.8	0.2	5.2	
Max	7.4	10.2	8.1	16.0	32.5	8.5	14.3	16.9	46.1	72.0	8.8	26.7	21.4	1.7	12.5	
Min	0.0	0.0	0.0	0.5	0.0	0.0	0.0	0.0	7.1	1.6	0.0	0.0	0.0	0.0	0.6	
SD	2.0	2.7	2.4	4.7	10.1	1.9	4.3	3.9	9.0	24.0	3.2	6.5	4.8	0.4	3.9	
FLUXES (shells m^{-2} d^{-1})																
Mean	7.9	10.2	13.2	19.6	15.8	3.6	12.0	11.0	113.8	354.9	3.3	57.2	5.3	1.8	24.8	629.8
Max	26.1	47.8	34.7	65.7	127.4	21.7	28.7	35.0	368.5	1361.5	22.3	482.0	34.7	13.0	182.4	1889.9
Min	0.0	0.0	0.0	3.2	0.0	0.0	0.0	0.0	3.2	3.2	0.0	0.0	0.0	0.0	3.0	44.6
SD	6.5	11.1	11.3	17.7	29.6	5.8	8.6	10.7	107.2	426.4	6.3	110.7	8.8	3.9	39.9	

352
353 A total of 3723 planktonic foraminifera shells and 141 benthic foraminifera were counted.
354 Planktonic foraminifera were identified at the species level, resulting in a total of 15 different species
355 identified (Plate 1). A mean of 196 planktonic foraminifera specimens per sample were identified,
356 with a minimum of 14 individuals in November 2013 and a maximum of 633 individuals in mid-
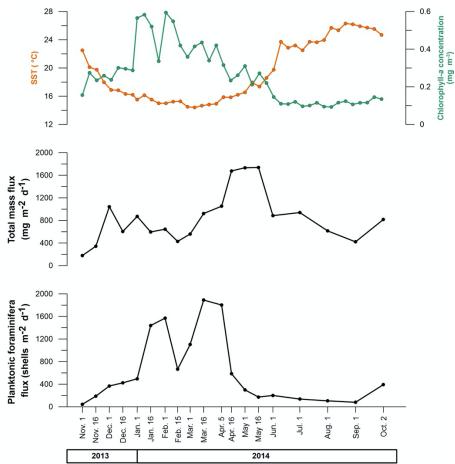357 March 2014 (Table 1).
358 According to the raw counts results, the most abundant species was *G. inflata*, which represented
359 55.7% of the total planktonic foraminifera individuals. The second most represented species was *G.
360 truncatulinoides*, with 18.9%, followed by *G. bulloides* with 8.2%. These three species alone
361 accounted for more than 80% of the planktonic foraminifera identified. The remaining species
362 abundances were below 5%. *G. ruber*, *G. ruber* (pink), *O. universa*, *G. rubescens* and *G. sacculifer*
363 represented between 2 and 3.3 % of the total individuals. Species like *G. tenella*, *G. scitula*, *N.
364 incompta* and *T. quinqueloba* were very scarce and accounted individually for less than 1% of the
365 total planktonic individuals (Table 1). Finally, only one individual of *G. falconensis* has been
366 identified. Note that *G. inflata*, *G. truncatulinoides* and *G. ruber* were the only species present in all
367 samples. Concerning the differentiation between lobulated and sac-type *Globigerinoides*, we mainly
368 found individuals belonging to the first group, the sac-type individuals were scarce. The latter were
369 identified mainly during summer and autumn.

370 Finally, the benthic foraminifera only represented 3.3% of the total foraminifera identified and 80%
371 of the individuals were identified in the two samples retrieved during April 2014 (see Supplementary
372 data).
373
374 **4.2 Total mass and planktonic foraminifera fluxes**
375

376
377 **Figure 2.** Total mass flux (TMF) (mg m^{-2} day^{-1}), total planktonic foraminifera flux (PFF) (shells m^{-2} day^{-1}),
378 SST (°C) and chlorophyll-a concentration (mg m^{-3}) changes between November 2013 and October 2014.
379
380 The mean total mass flux for the whole period of the study was 772.5 mg m^{-2} d^{-1}, with a maximum
381 value of 1737.7 mg m^{-2} d^{-1} and a minimum value of 179.5 mg m^{-2} d^{-1} reached in mid-May 2014 and
382 November 2013 respectively (Figure 2). Higher total mass flux values were reached during spring
383 2014, while lower values appeared during both autumn 2013 and 2014.
384 Planktonic foraminifera mean flux across the interval studied was 629.8 shells m^{-2} d^{-1} with a
385 maximum value of 1889.9 shells m^{-2} d^{-1} and a minimum of 44.6 shells m^{-2} d^{-1} reached in mid-March
386 2014 and in November 2013 respectively. Higher values occurred during two periods, early spring
387 and winter 2014, while the lower ones occurred from late spring to fall 2014. Overall, the seasonal
388 mean values were 1194.3 shells m^{-2} d^{-1} for the winter period, 612.3 shells m^{-2} d^{-1} for spring, 283.5
389 shells m^{-2} d^{-1} for autumn and finally 107.2 shells m^{-2} d^{-1} for summer.

390 SST mean value was 19.2 °C and values ranged between a maximum of 26.1 and a minimum of 14.5
391 °C. The mean chlorophyll-*a* value was 0.27 mg m^{-3}, the maximum value displayed was 0.56 mg m^{-3}
392 while the minimum one was 0.09 mg m^{-3} (Figure 2).
393

394 **4.3 Foraminifera species fluxes**
395

396 Overall, most of the planktonic foraminifera species collected by the trap exhibited either a uni-
397 modal or bi-modal flux distribution with a few exceptions (Figure 3).
398 *Globorotalia inflata* exhibited the highest fluxes of all species, with a mean flux of 368 shells m^{-2} d^{-1}
399 throughout the record, with peak values in mid-March 2014 (1361 shells m^{-2} d^{-1}) and minimum in
400 November 2013 (3 shells m^{-2} d^{-1}). *G. truncatulinoides* was the second most important contributor
401 (mean of 114 shells m^{-2} d^{-1}), with a maximum in mid-February and a minimum in November 2013
402 (368 and 3 shells m^{-2} d^{-1}, respectively). *G. bulloides* was the third most important contributor to the
403 total planktonic foraminifera fluxes with a mean flux of 57.2 shells m^{-2} d^{-1} and maximum values
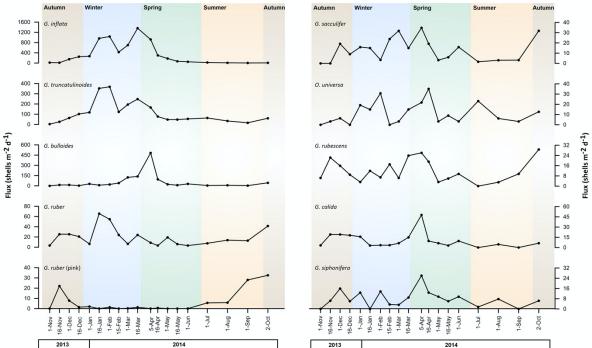404 registered in April 2014 and minima in November 2013 (482 and 0 shells m^{-2}d^{-1}, respectively).
405 The remaining species displayed mean fluxes lower than 50 shells m^{-2}d^{-1}. *G. calida*, *G. ruber*, *G. ruber*
406 (pink), *G. rubescens* and *O. universa* mean fluxes were comprised between 10 and 20. Among these
407 species, *G. ruber* and *G. ruber* (pink) stood out and showed maximum fluxes of 66 shells m^{-2} d^{-1} in
408 February 2014 and 127 shells m^{-2} d^{-1} in October 2014, respectively. The remaining species, *G.*
409 *siphonifera*, *G. scitula*, *N. incompta* and *T. quinqueloba* mean and maximum fluxes were lower than
410 10 and 35 shells m^{-2} d^{-1}, respectively, thereby representing a low contribution to the total
411 foraminifera fluxes.
412 Finally, it is worth noting that benthic foraminifera were also collected by the trap, displaying a mean
413 flux of 25 shells m^{-2} d^{-1}. The peak contribution of these taxa was recorded in April 2014 (182 shells
414 m^{-2} d^{-1}), and a minimum value in January 2014 (3 shells m^{-2} d^{-1}). In terms of annualized foraminifera
415 flux, their contribution was only a 1.1% of the total foraminifera identified of which 75% was
416 recorded during April 2014 (Figure 6).
417

Figure 3. Planktonic foraminifera fluxes (shells m^{-2} d^{-1}) from November 2013 to October 2014 of the 10 most abundant species identified. Note that the scale of the fluxes depend on the species. Background colour filling represents the different seasons: brown for autumn, blue for winter, green for spring and orange for summer.
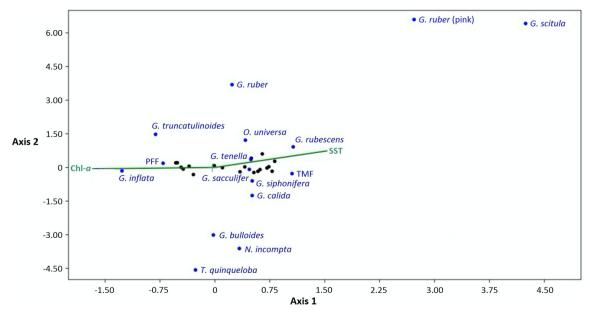
The variations in relative abundance differed according to the species. Most of the species displayed a unimodal distribution across the studied interval (Supplementary Figure 3), with some exceptions such as *G. siphonifera*, *G. calida* or *G. ruber*. Overall, *G. inflata* dominated the association from late autumn until mid-spring. *G. truncatulinoides* relative abundance pattern was similar to that of *G. inflata*, with maximum values in autumn and late summer. In turn *G. bulloides*, displayed a pronounced seasonal change in its relative abundance reaching values up to 27% in early spring (April 2014) and dropping to about 5-8% in November 2014.

Overall, *G. inflata* is the only species that displayed its maximum mean relative abundance during winter: 64%. *G. siphonifera*, *G. sacculifer*, and *G. bulloides*, maximum mean relative abundances were reached during spring: 3%, 3.5%, 14% respectively. *G. calida*, *G. tenella*, *G. rubescens* and *N. incompta* maximum mean abundances appeared to be in autumn: 5.7%, 2.2%, 8% and 4.8% respectively. Finally, *G. ruber*, *G. ruber* (pink), *O. universa*, *G. truncatulinoides* and *G. scitula* maximum mean relative abundances were displayed in summer: 11.6%, 13.2%, 8.9%, 32.8% and 6.4% respectively (Supplementary Figure 3).

4.4 Chlorophyll-*a* and SST impact on foraminifera fluxes

14

Figure 4. CCA analysis of all the planktonic foraminifera species flux with the SST (°C) and the chlorophyll-*a* ("chl-*a*" in the CCA, in mg m^{-3}) as the explanatory variables. The total mass flux ("TMF") and planktonic foraminifera flux ("PFF") are also included. Black dots represent the 19 sediment trap samples studied.

A CCA (see section 3.4) was carried out to characterize the impact of both the SST and the chlorophyll-*a* on the planktonic foraminifera fluxes (Figure 4).

Axis 1 shows, overall, the differences between deep and surface dwellers. Total planktonic foraminifera flux (PFF) and the fluxes of *G. inflata* and *G. truncatulinoides* are positively affected by the chlorophyll-*a* concentration and negatively affected by the SST. On the other hand, *G. ruber*, *G. ruber* (pink) and *G. scitula* fluxes showed an opposite pattern, being positively related with the SST and negatively with the chlorophyll-*a* concentration. *O. universa*, *G. rubescens*, *G. tenella*, *G. sacculifer*, *G. siphonifera* and *G. calida* fluxes are positively correlated with the SST and negatively with chlorophyll-*a* concentration, nonetheless, the impact of these parameters is weaker compared with the previous species. Finally, *G. bulloides*, *N. incompta* and *T. quinqueloba* fluxes are slightly positively influenced by the chlorophyll-*a* concentration, however. Axis 2 tends to separate the species between the different trophic regimes. Overall, it confirms that, in the one hand, *G. ruber*, *G. ruber* (pink) and *G. scitula* display a strong negative correlation with chlorophyll-*a* and therefore an affinity for oligotrophic and warm conditions; and on the other hand, shows that *G. bulloides*, *N. incompta* and *T. quinqueloba* display a positive correlation with chlorophyll-*a* and eutrophic conditions. Furthermore, *G. bulloides* flux shows a strong correlation with the latter two species: 0.89 and 0.83 ($p < 0.05$).

5. Discussion

5.1 Seasonal variations in the magnitude of planktonic foraminifera fluxes in the Sicily Channel

15

468 The strong seasonality in the planktonic foraminifera fluxes registered by the trap is generally similar
469 in amplitude to previous studies in the Mediterranean (Bárcena et al., 2004; Rigual-Hernández et
470 al., 2012) and other temperate settings (Kuroyanagi and Kawahata, 2004; Wilke et al., 2009),
471 thereby suggesting the C01 record mainly reflects the temporal variations in planktonic foraminifera
472 abundance in the upper water column. Therefore, next, we discuss the influence of oceanographic
473 controls on the planktonic foraminifera fluxes.
474 Our data shows that, despite differences in the magnitude of their fluxes, most of the species
475 identified display their maximum flux during winter, winter/spring transition or spring (Figure 3)
476 thereby coinciding with the period of maximum algal biomass accumulation and coldest SSTs (Figure
477 2). The enhanced primary productivity during winter and spring is mostly related to an
478 intensification of the chlorophyll-*a* and nutrient richer MAW flow into the Eastern Mediterranean
479 basin (D'Ortenzio, 2009; Pinardi et al., 2015; Siokou-Frangou et al., 2010). Our CCA results (Figure 4)
480 show that, although the flux patterns increase during winter and spring, only the planktonic
481 foraminifera flux, *G. inflata*, *G. truncatulinoides* and arguably *G. bulloides* (further discussed below)
482 fluxes are negatively related to SSTs and positively with the chlorophyll-*a* concentration. The
483 dominance of the planktonic foraminifera fluxes by these three species and their affinity for
484 mesotrophic waters is not surprising as *G. inflata* and *G. truncatulinoides* are typically associated
485 with the MAW, winter water mixing events and hydrologic fronts in the western Mediterranean,
486 while *G. bulloides* is generally associated with eutrophic environments linked to upwelling
487 conditions (Azibeiro et al., 2023). Overall, these three taxa have been described to be dominant
488 during winter in various western regions of the Mediterranean, such as the Alboran Sea (Bárcena et
489 al., 2004; Hernández-Almeida et al., 2011), the Provençal basin and in the Gulf of Lions (Pujol and
490 Grazzini, 1995; Rigual-Hernández et al., 2012). Interestingly *G. inflata*, *G. truncatulinoides* and *G.*
491 *bulloides* are almost absent in the eastern part of the basin, most likely due to the low algal biomass
492 accumulation (Avnaim-Katav et al., 2020; Thunell, 1978).
493 Conversely, species such as *G. ruber*, *G. ruber* (pink), *G. scitula*, *G. rubescens* and *G. sacculifer* display
494 their maximum fluxes in summer or autumn (Figure 3). During the warm periods, summer and
495 autumn, the eastward advection of Atlantic waters in the Sicily Channel is weakened due to an
496 increased meandering of the ATC (Figure 1) and the local hydrography patterns (Béranger et al.,
497 2004), leading to a local water column stratification period which is also well documented in the
498 whole Mediterranean basin during summer (Siokou-Frangou et al., 2010). This translates into a
499 reduced MAW influence, and a larger influence of the LIW at intermediate depths (Astraldi et al.,
500 2002, 2001; Jouini et al., 2016). Therefore, the water column becomes warmer, saltier and more
501 nutrient depleted than the general conditions of the western basin (Gasparini et al., 2005; Navarro
502 et al., 2017; Siokou-Frangou et al., 2010) and provides the necessary environmental and
503 oceanographical configuration for eastern basins taxa to develop or being transported from the
504 easternmost part of the Mediterranean. Indeed, our CCA results (Figure 4) support these
505 observations (Figure 3). The latter species have been described to reach their maximum abundances
506 in the eastern part of the Mediterranean, specifically in the Ionian and Levantine basins during both
507 summer and autumn (Avnaim-Katav et al., 2020; Pujol and Grazzini, 1995).
508 Some species, such as *O. universa* or *G. calida*, do not display a clear flux pattern over the period
509 studied. CCA results suggest that these species have an affinity for warm and less productive

510 conditions. These taxa are considered widespread in the Mediterranean basin, although their
511 relative contributions are generally higher in the eastern part of the basin (Avnaim-Katav et al.,
512 2020; Pujol and Grazzini, 1995; Thunell, 1978). Lastly, it is important to note that the low number of
513 specimens of *G. falconensis*, *N. incompta*, *T. quinqueloba* and *G. tenella* found in our samples, makes
514 the estimation of shell fluxes for these species unreliable. These results are not surprising, since *N.*
515 *incompta* is mainly found in the northwestern part of the basin owing to cold and eutrophic
516 conditions (Azibeiro et al., 2023; Millot and Taupier-Letage, 2005) while *T. quinqueloba* has generally
517 been associated to cool Atlantic waters or cool marginal seas (Azibeiro et al., 2023).
518 In summary, planktonic foraminifera flux was maximum during winter and spring, coinciding with
519 the maximum seasonal eastward advection that brings MAW further east into the Sicily Channel.
520 These waters are less saline and nutrient enriched compared to the easternmost waters from the
521 Levantine basin. *G. inflata*, *G. truncatulinoides* and *G. bulloides* (the three most abundant species
522 that dominate the PFF), which are species described to come from the western basins, are probably
523 brought by the MAW and then dominate the planktonic foraminifera population. On the other hand,
524 during summer and autumn, the eastward advection weakens, allowing the LIW and AIS to
525 dominate the surface circulation due to the water column stratification and set favourable
526 conditions for eastern basin dominant taxa such as both morphotypes of *G. ruber*, *G. rubescens*, *G.*
527 *sacculifer*. This results in a significantly decreased planktonic foraminifera flux due to the absence
528 of western basin dominant species.
529
530 **5.2 Species succession, ecology and impact of the SST and chlorophyll-*a***
531
532 The time series of settling planktonic foraminifera reflects a diverse assemblage with species with
533 contrastingly different ecological preferences, encompassing a wide range of depth habitats and
534 diverse feeding strategies. Overall, the annual assemblage composition agrees well with previous
535 ship-board observations (Pujol and Grazzini, 1995) in the Channel of Sicily during VICOMED 1988
536 cruise, where *G. inflata*, *G. truncatulinoides* and *G. bulloides* were documented as the most
537 abundant taxa.
538 Next, we discuss the ecology of the most abundant species and the impact of chlorophyll-*a* and SST
539 on their distribution. We also discuss the foraminifera groups suggested by Jonkers and Kučera,
540 (2015), to explore their correlation with the previous parameters on an interannual scale. The latter
541 work proposed 3 groups: group 1 is formed by tropical and subtropical species, group 2 consists of
542 temperate to subpolar taxa, and group 3 represents the deep-dwelling species. These groups were
543 described as a result of the seasonal maximum fluxes timing of each species and their relationship
544 with both temperatures and nutrients (amongst other parameters) in different time-series across
545 the world ocean. Therefore, here we also used this grouping to compare and complete this
546 classification from a new time-series dataset.
547 *Globorotalia inflata* is the most abundant taxon in our samples. Our data shows that maximum
548 fluxes and relative abundances of this species are reached during winter and the winter-spring
549 transition (Figure 3). The relative abundances showed strong positive and negative significant (p
550 <0.05) correlations with the chlorophyll-*a* concentration and the SST: 0.808 and -0.896 respectively
551 (Figure 5). It is a non-spinose species and is considered a deep dweller (Hemleben et al., 1989;

17

552 Schiebel and Hemleben, 2017). Generally regarded as showing limited opportunistic behaviour and
553 it has been often associated with eddies and hydrological fronts (Chapman, 2010; Retailleau et al.,
554 2011). Concerning the Mediterranean, its maximum stocks and abundances have been recorded
555 along the southern margin of the western Mediterranean basin (Azibeiro et al., 2023), especially
556 during winter (Bárcena et al., 2004; Pujol and Grazzini, 1995; Rigual-Hernández et al., 2012); while
557 it is poorly represented in the eastern part, even absent in the Levantine basin (Avnaim-Katav et al.,
558 2020). As a consequence, *G. inflata* can be considered as a mesotrophic species, which is dominant
559 in regions with some degree of stratification of the water column and an intermediate amount of
560 nutrients and it has been used as a tracer of the Atlantic inflow in the Mediterranean basin (Azibeiro
561 et al., 2023), which agrees with the local hydrography in the Sicily Channel during winter and spring.
562 As *G. inflata* appeared in periods of cool and nutrient enriched waters (Figure 3), which coincide
563 with the periods of higher MAW influence in the Sicily Channel (Béranger et al., 2004), we consider
564 that our results further confirm *G. inflata* as tracer of the MAW in the Sicily Channel.
565 *Globorotalia truncatulinoides* is the second most abundant species in our record. However, our CCA
566 results suggest that the seasonal variations in *G. truncatulinoides* are not directly correlated with
567 either chlorophyll-*a* concentration or SSTs (r= -0.162 and 0.256, respectively, *p* >0.05) (Figure 5).
568 This highlights the fact that environmental controls other than the ones considered here may be
569 affecting its distribution. This taxon is a cosmopolitan species found in all major oceans (Schiebel
570 and Hemleben, 2017) and is considered a deep dweller with an affinity for water-mixing conditions
571 (Margaritelli et al., 2020; Schiebel and Hemleben, 2005). It is a non-spinose species with a complex
572 life cycle. In the Mediterranean, peak abundances of this species are found in the northwestern part
573 of the basin, where it represents a major component of the assemblages (Pujol and Grazzini, 1995;
574 Rigual-Hernández et al., 2012), while it is absent in the easternmost part of the basin (Avnaim-Katav
575 et al., 2020). This species has been documented to have a complex life cycle and reproductive
576 strategy. *G. truncatulinoides* has been described to reproduce once a year in the upper layers of the
577 water column, generally when the water mixing allows the migration of juvenile individuals to the
578 surface (Lohmann and Schweitzer, 1990; Schiebel et al., 2002). Then, adult individuals migrate
579 downward the water column and spend the rest of their life cycle (Rebotim et al., 2017; Schiebel
580 and Hemleben, 2005). Hence, we speculate that these complex migratory patterns may be playing
581 a role here. As its reproduction cycle is mainly controlled by the gametogenesis process, and as
582 described previously, it reproduces once a year (a slower rate than the majority of the planktonic
583 foraminifera species) (Schiebel and Hemleben, 2017), then, although different stages of its life cycle
584 could be affected by SST and chlorophyll-*a*, this is not necessarily registered by the sediment traps
585 in every stage of its growth.
586 *Globigerina bulloides* was the third most abundant planktonic foraminifera species identified here.
587 It is a surface to subsurface dweller and one of the most common species across the world ocean
588 (Schiebel and Hemleben, 2017). Interestingly, our analysis showed no significant correlation
589 between changes in *G. bulloides* relative abundance and chlorophyll-*a* concentration or SST (r= -
590 0.145 and -0.111 respectively, *p* >0.05). However, across the time span studied, this taxon showed
591 its maximum abundance and fluxes during relatively high chlorophyll-*a* and cool SST conditions
592 (Figure 3). This highlights that other environmental parameters than the ones considered here might
593 be playing a role in its distribution. It is a spinose species known for its opportunistic feeding strategy

594 (Schiebel et al., 2001) and affinity for upwelling and eutrophic environments (Azibeiro et al., 2023;
595 Bé et al., 1977). Within the Mediterranean Sea, it displays peak export fluxes to the deep sea in
596 areas of high productivity such as the Gulf of Lions and the Alboran Sea during the high productivity
597 period in late winter to spring (Azibeiro et al., 2023; Bárcena et al., 2004; Hernández-Almeida et al.,
598 2011; Rigual-Hernández et al., 2012), while few individuals are found in the eastern part of the
599 Mediterranean (Avnaim-Katav et al., 2020). We surmise that owing to its multiple trophic strategies
600 and its multi-diet characteristics, it could adapt and feed on varying chlorophyll-*a* concentrations.
601 Also, the lack of correlation with both parameters could be explained by the fact that this taxon is
602 associated with eutrophic conditions. In the Sicily Channel, the high productivity period ranges from
603 winter to spring, and the conditions allow deep mesotrophic dwellers (i.e. *G. inflata*) to dominate
604 the assemblage; while in summer and autumn, the upwelling setting brings oligotrophic conditions
605 that are not favourable for this species.

606 Generally, both *G. bulloides* and *G. truncatulinoides* fluxes and abundances are positively linked to
607 favourable food conditions and high-productivity environments. The first species tends to exhibit a
608 "bloom" strategy on short time scales, while the second species tends to be related to nutrient
609 advection zones in the Mediterranean Sea (Margaritelli et al., 2022). Furthermore, in the
610 Northwestern Mediterranean a previous study showed that the fluxes of these two species are
611 almost in phase (Rigual-Hernández et al., 2012). Interestingly, in the Sicily Channel, this relation is
612 not straightforward. In the Gulf of Lions, *G. bulloides* is the main species and shows the classical
613 "bloom" behaviour, while *G. truncatulinoides* pattern is more constant and its variations are more
614 gradual (Rigual-Hernández et al., 2012). Although the timing of the two species is different in our
615 record, the response of *G. truncatulinoides* is similar across the record. Furthermore, from a
616 productivity standpoint, the Sicily Channel is less productive than the Gulf of Lions (Siokou-Frangou
617 et al., 2010), which, in turn, does not benefit *G. bulloides* abundances and, as the upwelling in our
618 study zone is less pronounced than in other parts of the Mediterranean, the timing between the
619 two species is different. Additionally, the intensity of the upwelling in the central Mediterranean is
620 controlled by variations in the intensity of the LIW flowing to the western part of the basin (Astraldi
621 et al., 2001; Lermusiaux and Robinson, 2001; Pinardi et al., 2015), with higher intensity leading to
622 reduced upwelling and therefore, productivity. This could explain the lack of high abundance of *G.*
623 *bulloides* in our study region as the upwelling in the Sicily Channel is reduced compared to other
624 places in the Mediterranean (D'Ortenzio, 2009; Siokou-Frangou et al., 2010) and therefore, the
625 increase in productivity is diminished compared to other regions in which the productivity and the
626 abundance of *G. bulloides* are higher, such as the Alboran Sea (Bárcena et al., 2004). Therefore, we
627 consider that a combination of ecological preferences and oceanographic processes could explain
628 the lack of synchronicity between these two species fluxes and abundances.

629 *Globigerinoides ruber* and *G. ruber* (pink) were the fourth and fifth most abundant species in our
630 samples (Table 1). Our correlation analyses showed a significant positive effect of SST (r= 0.803 and
631 0.678, *p* <0.05) and a significant negative effect of chlorophyll-*a* (r= -0.567 and -0.464 respectively,
632 *p* <0.05) on both *G. ruber* and *G. ruber* (pink) respectively (Figure 5). These species have been
633 described as tropical to subtropical taxa, with an affinity for oligotrophic and stratified waters (Bé
634 et al., 1977). Both of these species are among the shallowest dwellers of the extant planktonic
635 foraminifera species and are considered one of the most adaptable to varying surface water

636 conditions (Kemle-von Mücke and Oberhänsli, 1999; Schiebel and Hemleben, 2017). Due to its
637 temperature and salinity limits for food acceptance, the white variety is one of the most studied
638 foraminifera species in culture experiments, which highlight their euryhaline and eurythermal life
639 cycle (Bijma et al., 1990; Lombard et al., 2009). In today's ocean, the white variety is substantially
640 more abundant than the pink one (Schiebel and Hemleben, 2017). In the case of the Mediterranean
641 basin, *G. ruber* is generally associated with warm and oligotrophic waters (Pujol and Grazzini, 1995)
642 and is abundant in the eastern oligotrophic basin, where it dominates the assemblages in the
643 Levantine basin during spring and fall (Avnaim-Katav et al., 2020). However, although present in the
644 western basin, its abundance is much lower in the Gulf of Lions (Rigual-Hernández et al., 2012) and
645 in the Alboran Sea (Bárcena et al., 2004). Overall, the correlation data agrees with the previous work
646 that linked *G. ruber* (both varieties) to warm and oligotrophic conditions generally displayed during
647 a higher stratification of the water column (Schiebel et al., 2004). As this species is mostly abundant
648 in the eastern part of the Mediterranean , it should be expected that the LIW, when it dominates
649 the circulation during summer and autumn, brings this species along with other oligotrophic taxa.
650 However, fluxes (Figure 3) and relative abundance data (supplementary Figure 3) showed that this
651 species maximum appearances were recorded during winter, coincidently with *G. inflata* and *G.*
652 *truncatulinoides*. Therefore, the winter recorded in our dataset showed favorable conditions for
653 both deep mesotrophic dwellers and oligotrophic species such as *G. ruber*. We interpret this pattern
654 as a reduced influence of the MAW during winter in the Sicily Channel that could lead to slightly
655 warmer than usual surface conditions that favor the stratification and hence, the *G. ruber*
656 abundances. Concerning *G. ruber* (pink), as its fluxes and abundances were higher during summer,
657 and it is mainly identified in the eastern part of the Mediterranean as well, we consider that the LIW
658 influence bring this species in the Sicily Channel.
659 According to Jonkers and Kučera, (2015), the foraminifera fluxes can be predicted on a seasonal
660 scale for three different groups of planktonic foraminifera. Following this approach, we explore the
661 relative abundance of these three aggrupations to document if these correlate with both SST and
662 chlorophyll-*a* concentration (see Supplementary Table 1) on the period covered by the sediment
663 trap (Figure 5). The first group (group 1) consists of both *G. ruber* varieties, *G. sacculifer*, *O. universa*,
664 *G. siphonifera*, *G. rubescens* and *G. tenella*. The second group (group 2) is formed by *G. bulloides*, *T.*
665 *quinqueloba*, *N. incompta*, *G. scitula* and *G. calida*. In our record, however, either *G. bulloides* or *G.*
666 *calida* displayed a similar trend, and the remaining three species abundance was <1.5%, making any
667 significant assumption difficult (Table 1). The third (group 3) is composed by the deep dwellers *G.*
668 *inflata* and *G. truncatulinoides*. Group 1 showed a strong and significant positive correlation with
669 the SST (Figure 5) and a negative with the chlorophyll-*a* (r= 0.828 and -0.668 respectively, *p* <0.05,
670 see Supplementary Table 1). This is not surprising as the majority of the group is formed by species
671 not only considered tropical but also well adapted to oligotrophic and nutrient impoverished
672 environments (Chapman, 2010; Hemleben et al., 1989; Schiebel and Hemleben, 2017). In addition,
673 most components of this group are symbiont bearing species (Takagi et al., 2019), which have been
674 described to be more adapted to nutrient depleted and oligotrophic conditions. Group 2 on the
675 other hand did not show any strong correlation to either SST and chlorophyll-*a* concentration,
676 although a significant negative correlation was displayed between the group abundances and the
677 latter parameter (r= -0.525, see Supplementary Table 1). This result is not surprising as the main

678 component of this group is *G. bulloides*, which previously showed a lack of correlation with both SST
679 and chlorophyll-*a*, while the remaining species of this group were taxa that tend to be outnumbered
680 by more opportunistic species (i.e. *N. incompta* and *T. quinqueloba*) (Kuroyanagi and Kawahata,
681 2004; Schiebel, 2002). Also, the overall abundance of these taxa was very low in our samples
682 compared to the other two groups, which in turn could affect the correlation results. Here we
683 propose that the mesotrophic conditions of the Sicily Channel developed during the relatively high
684 productivity period are not favourable enough for the development of the taxa comprised in group
685 2. Finally, group 3 displayed a strong and significant positive correlation with chlorophyll-*a*
686 concentration (r= 0.771, *p* <0.05), which is an expected trend according to the affinity showed to
687 mesotrophic conditions by the two species that constitute this group, however, as compared to
688 Jonkers and Kučera, (2015), we showed a strong and significant negative correlation of these two
689 species abundances with the SST (Figure 5). The latter work stated that the cycles of these species
690 were independent of the temperature changes, however, these two species tend to be used as
691 tracers of cool and deep mesotrophic waters in the Mediterranean, generally associated with the
692 MAW (Azibeiro et al., 2023).

693 In summary, our data showed that in the Sicily Channel, the three major ecological groups proposed
694 by Jonkers and Kučera, (2015), exhibited a different response to environmental variability. Overall,
695 groups 1 and 3 showed significant correlation with the latter parameters and were in accordance
696 with their corresponding species ecologies. However, group 2 did not show any significant
697 correlation, which we interpreted as the result of very low abundances of the taxa comprised within
698 this group. This translates into the dominance of group 1 during summer and autumn when
699 oligotrophic and warm eastern waters dominate the water column, while the mesotrophic taxa from
700 group 3 dominate during winter and spring, coincidently with higher primary productivity, yet not
701 eutrophic enough for the opportunistic taxa comprised in the group 2, which is less well represented
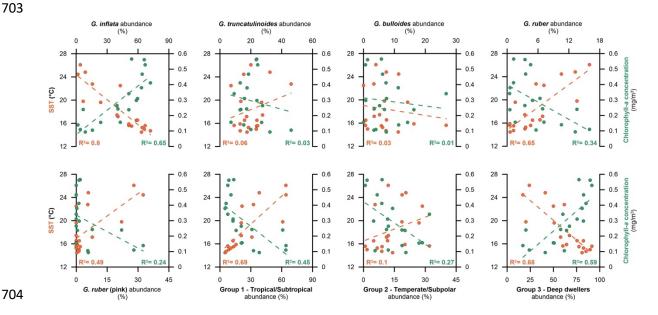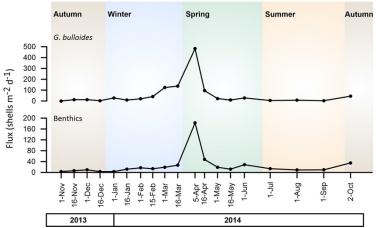702 in the Sicily Channel.

703

704

705 **Figure 5.** SST and chlorophyll-*a* concentration against the relative abundance of the five most abundant
706 species and the three ecological groups proposed by Jonkers and Kučera (2015). Orange dots stand for
707 SST while the green ones correspond to chlorophyll-*a*.

708 **5.3. Influence of the hydrodynamic conditions on the planktonic foraminifera assemblage**
709

710 A possible source of variability between the living foraminifera assemblages and those collected by
711 the trap could be the preferential transport of certain species by the currents as well as differences
712 in the sinking rates between species. Typically, deep dwelling species produce heavier shells that
713 the surface dwelling ones (Zarkogiannis et al., 2022). Theoretically, lighter species are easier to
714 remobilize than the heavier ones, however, if the current is strong enough, lighter species could
715 travel far away while heavier species could be reworked in the vicinity of their deposition zone. *G.*
716 *truncatulinoides* is among the heaviest planktonic foraminifera species (Beer et al., 2010; Béjard et
717 al., 2023). Therefore, if the current is strong enough, it could be resuspended and be recorded by
718 the sediment trap. The record in the seabed sediment (see section 5.5) showed that *G.*
719 *truncatulinoides* was more abundant in the settling particles from the C01 mooring line (Figure 8),
720 and according to the winnowing theory, *G. inflata* should follow a similar pattern as it also a heavy
721 species (Zarkogiannis et al., 2022). However, surface data (Mallo et al., 2017) showed that the latter
722 is also the dominant species in the BONGO nets (see section 5.5). Furthermore, Takahashi and Be,
723 (1984) presented the data about the sinking speeds of different planktonic foraminifera species. As
724 an example, *G. inflata* showed a sinking speed of 500 m per day, compared to 330 m per day for *G.*
725 *bulloides*. These different sinking rates applied in a water column of around 450 m suggest that the
726 likely origins of the planktonic foraminifera collected by the traps must be similar and are insufficient
727 to generate discrepancies between the foraminifera assemblages living in the upper water column
728 and those collected by the trap.
729

731 **Figure 6.** *G. bulloides* and benthic foraminifera fluxes (shells m^{-2} d^{-1}) between November 2013 and
732 October 2014.
733

734 The identification of benthic foraminifera individuals highlights suggest an impact of the
735 hydrodynamic conditions on the settling particles populations. The main species identified were *T.*
736 *saggitula* spp. and *B. marginata* (Plate 1) along with a small number of *Uvigerina mediterranea* and

Lagenina striata. These taxa are considered infaunal species, i.e. they live buried in the sediment (Balestra et al., 2017; Milker and Schmiedl, 2012) and are commonly found in continental shelves and slopes. Overall, benthic foraminifera accounted only for a mean of 3.4% of the total foraminifera identified in the C01 settling particles (Table 1) and the percentage of planktonic oscillated between 89 and 99.4%. Most of the annual benthic fluxes occurred during April, when a total of 80% of the annual benthic foraminifera fluxes were recorded (Figure 6). As described previously, the Sicily Channel hydrography is complex from both a vertical and seasonal point of view (Astraldi et al., 2001; Garcia-Solsona et al., 2020; Incarbona et al., 2011; Pinardi et al., 2015; Schroeder et al., 2017). In the Sicily Channel, the tidal and subtidal current speed is known to reach maximum annual values during the spring period (Gasparini et al., 2004) which could be invoked as a possible source of sediment resuspension including benthic species. This has also been observed in different parts of the Mediterranean (Grifoll et al., 2019). Indeed, in our record, the highest benthic foraminifera fluxes were collected during spring (Figure 6), i.e. the period of peak current intensity in the Channel. Coincidently, it also showed the highest fluxes of *G. bulloides* (Figure 3), which is the third most abundant species in our record (Table 1). Interestingly, this species annual flux distribution showed no correlation with either the SST nor the chlorophyll-*a* (Figure 5). These observations, coupled with the fact that the fluxes of *G. bulloides* and the benthic foraminifera were positively and significantly correlated (r= 0.89, *p*<0.05), suggest that benthic species were resuspended, being caught at 40 m of water depth by our sediment trap. Furthermore, a low number of detritic debris, such as mica flakes, were identified in the samples that contained the highest number of benthic foraminifera (April 2014), which again suggest a secondary influence of resuspended sediments in the sediment trap record in specific intervals of the annual cycle. However, no such relationship has been identified with the other species that did not show any correlation with the previous environmental parameters: *G. truncatulinoides*. Consequently, we hereby propose that *G. bulloides* distribution and abundances are blurred in specific intervals by the resuspension of sea floor sediments. Finally, the increase of *G. bulloides* abundance and fluxes that has been identified coincidently with a higher number of benthic foraminifera during early April could lead to the interpretation that the benthic foraminifera are the result of the intensification of the MAW. However, as the presence of the benthic foraminifera is patchy and not constant, we do not consider their presence is ruled out as a reliable proxy for the MAW/LIW intensity. Therefore, it can be concluded that the C01 sediment trap mainly records a pelagic signal with a secondary influence of resuspended sediments.

5.4 Geographical variability in the magnitude and composition of planktonic foraminifera fluxes across the Mediterranean

The comparison of the settling planktonic foraminifera assemblage from the Sicily Channel with the ones retrieved from different parts of the Mediterranean offers a unique opportunity to provide further insight into the central Mediterranean dynamics and ecology of this group.

As stated previously, the planktonic foraminifera flux in the Sicily Channel was higher from mid-January to mid-March, which coincided with the highest chlorophyll concentrations and the coolest SST recorded (Figure 2). This seasonality is similar to the one observed in the Gulf of Lions, where the planktonic foraminifera flux reached its highest values from mid-February to mid-March during

779   different years (Rigual-Hernández et al., 2012). Although slightly different, the planktonic
780   foraminifera fluxes patterns from both the Levantine basin and the Alboran Sea also displayed
781   maximum values between mid-February to mid-March and mid-January to mid-February
782   respectively (Avnaim-Katav et al., 2020; Hernández-Almeida et al., 2011). However, the magnitude
783   of the planktonic foraminifera flux values displayed some differences between the sites (see
784   Supplementary Figure 2). Overall, for the Sicily Channel, values ranged between 0-1889 shells m^{-2} d^{-1}
785   with a mean value of 629 shells m^{-2} d^{-1}. These values were comparable to the ones from the Gulf
786   of Lions: 0-2114 and 4268 shells m^{-2} d^{-1} with a mean value of 225.4 in Planier sediment trap to 419
787   shells m^{-2} d^{-1} in Lacaze-Duthiers sediment trap (Figure 7). On the other hand, the Levantine basin
788   values were lower: 0-429 shells m^{-2} d^{-1}, with a mean value of 93 shells m^{-2} d^{-1}. Finally, the highest
789   values belonged to the Alboran Sea: 0-6000 shells m^{-2} d^{-1} with a mean value of 783 to 970 shells m^{-2} d^{-1}
790   depending on the gyres. Note that the planktonic foraminifera flux values from the Levantine
791   basin used here represent the foraminifera shells from the >125 μm fraction, which highlights the
792   fact that compared to the >150 μm, the flux values should be even lower. The corresponding
793   chlorophyll-*a* values registered in the latter sites were 0.2-0.65 mg m^{-3} for the Sicily Channel (Figure
794   5), 0.25-0.85 mg m^{-3} for the Gulf of Lions (0-0.65 mg m^{-3} in the Planier site, 0.25-0.85 mg m^{-3} for
795   Lacaze-Duthiers) (Rigual-Hernández et al., 2012), 0.02-0.4 mg m^{-3} for the Levantine basin (Avnaim-
796   Katav et al., 2020) and 0.1-1.2 mg m^{-3} in the Alboran Sea (Hernández-Almeida et al., 2011), indicating
797   a similar productivity in terms of chlorophyll-a between the Gulf of Lions and the Sicily Channel. In
798   addition, here we calculated an annualized planktonic foraminifera flux (section 3.4) for each of the
799   6 sites compared here (Figure 7). Overall, the highest annualized fluxes were displayed in the
800   Alboran Sea (Figure 7): around $3x10^5$ and $4.4x10^5$ shells m^{-2} y^{-1}, while the lowest one was displayed
801   in the Levantine Basin: a little over 30000 shells m^{-2} y^{-1} (Figure 7). The Gulf of Lions and the Sicily
802   Channel displayed comparable annualized fluxes although higher for the latter: around $1.5x10^5$ and
803    $1.85x10^5$ shells m^{-2} y^{-1} respectively. Note that PLA site values were significantly lower: around $7x10^4$
804   shells m^{-2} y^{-1} (Figure 7). Previous work showed that these planktonic foraminifera patterns were
805   mainly linked to specific regional oceanographic processes. First of all, the Levantine basin is well
806   known for being an ultra-oligotrophic region and being the warmest and saltiest of the
807   Mediterranean basins (Ozer et al., 2017), mainly due to the W-E anti-estuarine circulation. On the
808   other hand, the Gulf of Lions is considered an exception to the general oligotrophy of the
809   Mediterranean. Seasonal vertical mixing phenomenon occurs in winter, generated by cold winds.
810   This winter mixing recharges the surface waters with nutrients, allowing a winter/spring productivity
811   bloom (Durrieu de Madron et al., 2013; Houpert et al., 2016). Finally, the Alboran Sea is a transitional
812   region between the Atlantic Ocean and the Mediterranean Sea (Hernández-Almeida et al., 2011),
813   and unlike the latter, is not an oligotrophic region due to the two systems of high productivity
814   related to the gyres generated by an intense westerlies activity, which allow nutrients enriched
815   (compared to the resident waters) Atlantic waters to spread into the Mediterranean. This results in
816   an enhanced primary productivity period from November to March. According to the PFF patterns
817   displayed in this study, the Sicily Channel presents similar values and fluxes distributions to the Gulf
818   of Lions, however, its oceanographic circulation is significantly different from the latter. These
819   observations agree with the work of Mallo et al., (2017) carried out with plankton tows in the whole
820   Mediterranean basin. The latter work found that the Alboran Sea displayed the highest standing

821 stocks of planktonic foraminifera, while the easternmost part of the Mediterranean showed the
822 minimum values. Also, the Gulf of Lions and the Channel of Sicily displayed similar stocks, although
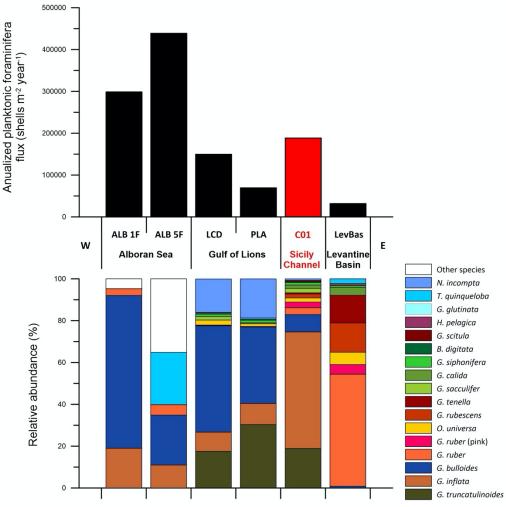823 slightly superior for the Channel of Sicily.

824
825 **Figure 7.** Comparison of the annualized (see section 3.4) planktonic foraminifera flux and the relative
826 abundance of each species identified in different time-series across the Mediterranean Sea (see section
827 3.5). The data from the Sicily Channel (C01) is depicted in red. Note that the Levantine Basin (LevBas)
828 dataset covers the >125 μm fraction. Other species (white bar) in the Alboran Sea corresponds to any
829 species different from the main 4 taxons identified in Bárcena et al., (2004) and Hernández-Almeida et
830 al., (2011).

831

832 Concerning the species composition, we identified 15 planktonic foraminifera species in the Sicily
833 Channel, which is a similar species number to the one from the Gulf of Lions (14 species) and higher
834 than in the Levantine basin (10 different species). The Sicily Channel site displayed the highest
835 planktonic foraminifera assemblage diversity among the three sites compared: a mean 1-D and S/W
836 index of 0.68 and 1.57 respectively. (Table 2). Interestingly, despite showing a similar number of
837 different species, the Gulf of Lions displayed the lowest diversity values, especially for the PLA site:
838 mean 1-D of 0.55 and mean H/W of 1.08, while the LCD site 1-D and h/w were 0.58 and 1.15

respectively. These observations highlight that, although the annualized planktonic foraminifera flux was similar between the Gulf of Lions (for the LCD site) and the Sicily Channel (Figure 7), the assemblage in the latter site was significantly more diverse regarding species composition. The composition of the annual planktonic foraminifera population of the different species showed some differences between the sites compared here. In the Levantine basin, the majority of the planktonic foraminifera population consisted of surface symbiont bearing species such as *G. ruber*, *G. ruber* (pink), *G. rubescens*, *G. tenella*, *O. universa*, which are well adapted to the ultra-oligotrophic conditions (Lombard et al., 2011; Schiebel and Hemleben, 2017). The latter species represented 96% of the total planktonic foraminifera in the Levantine basin, while the same species in the Sicily Channel accounted for around 10% of the total individuals (Figure 7). Note that both *G. rubescens* and *G. tenella* are considered small-sized species (Chernihovsky et al., 2023) and their adult size is often smaller than 150 µm, so it is possible that some individuals of those species may not be recorded in our data. On the other hand, in the Gulf of Lions, the four main species were *G. bulloides*, *N. incompta*, *G. inflata* and *G. truncatulinoides*, which represented 88 to 95% of the total planktonic foraminifera (Rigual-Hernández et al., 2012). These species tend to be associated with eutrophic to mesotrophic environments which coincides with the Gulf of Lions locally enhanced primary productivity conditions. In the Sicily Channel, the same species accounted for 83% of the total individuals, and, except for *N. incompta*, the remaining three species were also the most abundant in our samples.

Table 2. Inverse Simpson (1-H) and Shannon-Weiner indexes mean, standard deviation ("Stan. Dev.") and maximum values for the two Gulf of Lions sites (PLA and LCD), the Sicily Channel (C01, this study) and the Levantine Basin (LevBas).

	Gulf of Lions		Sicily Channel	Levantine Basin
	LCD	PLA	C01	LevBas
Simpson 1-H				
Mean	0.581	0.553	0.681	0.615
Stan. Dev.	0.168	0.180	0.132	0.144
Max	0.802	0.781	0.872	0.804
Shannon H/W				
Mean	1.151	1.078	1.572	1.230
Stan. Dev.	0.359	0.375	0.398	0.316
Max	1.789	1.630	2.188	1.759

Considering the planktonic foraminifera fluxes patterns, the species diversity and the planktonic foraminifera most abundant species from each of the three Mediterranean time-series with which we compared our data, we interpret that, from a planktonic foraminifera population point of view, the Sicily Channel could be considered as a transition zone and a biological corridor between the western and eastern basins.

869   Finally, to put our data into a global context, here we compare our dataset with planktonic
870   foraminifera data from the same size fraction retrieved in the Gulf of Mexico, high latitudes North
871   Atlantic and gyres region of the North Atlantic Ocean. In the northern Gulf of Mexico, from 2008 to
872   2010, the >150 μm PFF was comprised between 0 and slightly over 800 shells $m^{-2} d^{-1}$, with a mean
873   value of around 250 shells $m^{-2} d^{-1}$ (Poore et al., 2013). A total of 12 species were identified, with *G.
874   truncatulinoides*, *G. ruber* (pink) and *N. dutertrei* as the most abundant species recorded. On the
875   other hand, in the North and high-latitudes Atlantic Ocean, Wolfteich (1994), showed that the PFF
876   oscillated between 0 and around 5000 shells $m^{-2} d^{-1}$ for a mean value of 800 shells $m^{-2} d^{-1}$, while *G.
877   bulloides* and *N. incompta* were the most abundant species. Although the latter work only focused
878   on the most abundant species, additional work has documented more than 20 species in the vicinity
879   of the North-Atlantic gyres (Salmon et al., 2015), but around only three to four in the high latitudes.
880   This highlights that, from a planktonic foraminifera population point of view on a wider scale, the
881   Sicily Channel displayed a higher planktonic foraminifera flux and species richness compared to the
882   tropical to subtropical Gulf of Mexico and to the high latitudes of the North Atlantic, but lower values
883   compared to the North Atlantic gyres region.
884

885   **5.5 Recent planktonic foraminifera assemblage comparison with seabed sediment**
886

887   The Mediterranean Sea is often referred to as a climate change hotspot and a "laboratory basin" where
888   many global environmental trends are amplified (Bethoux et al., 1999). In particular, ocean warming is
889   expected to exceed the global average (Hassoun et al., 2022, 2015; Lazzari et al., 2014) while it is
890   considered a specially sensitive zone of the ocean to acidification due to the fast turnover of its waters
891   and penetration of anthropogenic CO_2 (Bethoux et al., 1999; Schneider et al., 2007). One of the main
892   questions about planktonic foraminifera concerns the way they are going to react to the ongoing climate
893   change in the global ocean (Jonkers and Kučera, 2015; Schiebel and Hemleben, 2017). Previous work
894   suggests that global communities of planktonic foraminifera have already been affected by
895   environmental change since the onset of industrialization (Jonkers et al., 2019). Moreover, recent work
896   has shown that the calcification of several planktonic foraminifera species has decreased during the
897   industrial era in the northwestern Mediterranean (Béjard et al., 2023). Therefore, here we aim to assess
898   if modern planktonic foraminifera communities dwelling in the Sicily Channel differ from their pre-
899   industrial counterparts. To do so, next, we compare the annual integrated assemblages collected by the
900   sediment trap in the C01 mooring line with the ones from a set of core-tops, two box-cores and BONGO
901   nets retrieved in the vicinity of the studied zone (see Section 3.5).
902   As planktonic foraminifera are a group of calcifying plankton, when comparing sediment trap and
903   seabed sediment data, the possible role of calcite dissolution must be discussed. Firstly, the
904   Mediterranean Sea is supersaturated with respect to calcite (Álvarez et al., 2014; Millero et al., 1979)
905   and the depth of the studied material is substantially shallower than the calcite saturation horizon
906   (Álvarez et al., 2014). Secondly, recent work suggests that calcite experiences little to negligible
907   changes in the water column and burial in recent sediments (Béjard et al., 2023; Pallacks et al.,
908   2023). All this evidence suggests that dissolution played a negligible role in the preservation of
909   planktonic foraminifera preserved in the sediment record in the study region.

910   The core-tops used for comparison were part of the MARGO database (see Section 3.5 for more
911   details). Note that the MARGO sites 3735 to 3739 seabed sediment was taken using a trigger-weight
912   corer (Thunell, 1978). However, samples 3658, 3672 and 3673 were retrieved using a piston corer
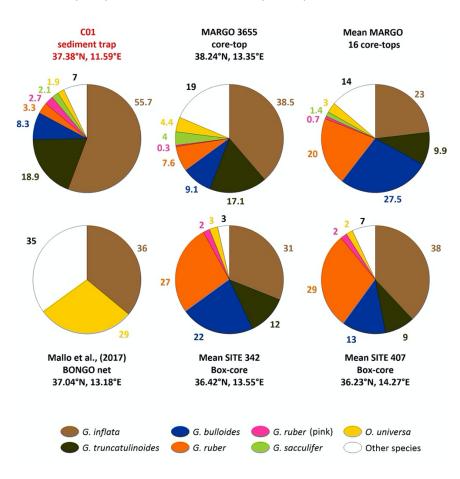913   (Hayes et al., 2005). Generally, sampling with the trigger-weight method is considered to retrieve
914   less mixed and disturbed sediment than the piston or box corer sampling methods (Skinner and
915   McCave, 2003; Wu et al., 2020). Therefore, the foraminifera assemblages from the core-tops may
916   likely represent a mix of Holocene populations rather than exclusively modern assemblages.
917   Although the lack of dating control makes it impossible to determine the exact date of the core top
918   assemblages.
919   The sites 342 and 407, studied by Incarbona et al., (2019), were retrieved with a box-corer. A total
920   of 23 and 24 samples were analyzed in the latter work, respectively. The advantage of comparing
921   the C01 assemblages with those of Incarbona et al., (2019) is the availability of high resolution [210]Pb
922   chronology. The ages ranged from 1718 to 1962 CE for site 342 and from 1558 to 1994 CE for site
923   407. Therefore, here we present a comparison with the mean relative abundance of the main
924   planktonic foraminifera species from all the samples available (Figure 8).
925   Finally, to provide a more complete snapshot of the surface assemblages, we also include the
926   abundances from Mallo et al., (2017) that were collected with a BONGO net during spring 2013 in
927   the axis of the Sicily Channel (Figure 8).
928   In terms of planktonic foraminifera assemblage composition, major differences were observed
929   between the different seabed sediments datasets (Figure 8). Overall, the settling population from
930   the C01 mooring line appeared to be closer to the assemblages from sites 342 and 407 (Figure 8)
931   than to the mean from the MARGO database (see Supplementary data). The most evident
932   observation relies on the shift of the dominant species when comparing the settling population with
933   the sites 342, 407, the BONGO net and the core-top assemblages (Figure 8). As described previously,
934   *G. inflata* dominated the assemblages collected by the sediment trap (Table 1). This is also the case
935   for the sites 342 and 407 and the BONGO net (Figure 8). However, *G. bulloides* was the best-
936   represented species in the core-tops from the MARGO database. Also, the second most abundant
937   species varied across the datasets: *G. ruber* in the sites 342 and 407, *O. universa* in the BONGO nets
938   and *G. inflata* in the MARGO core-tops, with abundances around 27-29, 29 and 27.5%, respectively.
939   Interestingly, *G. truncatulinoides* abundance was significantly lower in the seabed datasets and
940   absent in the BONGO nets, highlighting the deep aspect of its ecology (Figure 8). On the other hand,
941   the "other species" category, which consists of minor taxa such as *G. rubescens, G. siphonifera* and
942   *G. calida* (amongst others) played a more significant role in the MARGO core-tops and BONGO nets
943   assemblages, reaching abundances up to 26% (Figure 8), while in the sites 342 and 407, these
944   species abundances are similar to those of the sediment trap.
945   These results lead to several observations. Firstly, concerning the seabed sediment comparison, the
946   sediment trap assemblage is closer to the sites 342 and 407 than to the MARGO database core-tops.
947   The comparison with the surface BONGO nets shows that, although the dominant species are the
948   same (i.e. *G. inflata*), the influence of *O. universa* and the overall diversity is less important in surface
949   waters. This highlights the complexity of the Sicily Channel configuration and the differences
950   between the surface (BONGO nets), the water column (sediment trap) and the seabed sediment
951   (MARGO database and sites 342 and 407) regarding the planktonic foraminifera populations.

952 Secondly, the seabed sediment planktonic foraminifera populations showed a reduced influence of
953 deep-dwelling species (excepting for *G. inflata* in sites 342 and 407) and a more pronounced
954 influence of both eutrophic and oligotrophic species. These eutrophic species (such as *G. bulloides*
955 but also *N. incompta*) are associated with MAW and western basins in the modern Mediterranean
956 Sea, while the more oligotrophic taxa (*G. ruber*, *G. rubescens*, *G. calida*…) are considered to be
957 abundant in the easternmost part of the basin (Azibeiro et al., 2023). As noted previously, although
958 the settling assemblage differs to the ones from the seabed sediment, it is more similar to the sites
959 342 and 407 than to the MARGO database core-tops. Also, the ^{210}Pb chronology available for sites
960 342 and 407 covers the years 1558 to 1994 CE (Incarbona et al., 2019). A possible interpretation of
961 these results is that the MAW influence into the basin may have shifted. Instead of bringing rich and
962 eutrophic waters that would allow the development of opportunistic species, it nowadays brings
963 more mesotrophic water masses that favour the development of deep dwellers in the Sicily Channel.
964 On the other hand, this could also lead to the assumption of a reduced eastward and LIW influence
965 in the present day as seen by the significantly lower abundance of oligotrophic species in the settling
966 assemblages. Also, a change in the environmental conditions could lead to the increase of deep
967 dwellers in substitution of eutrophic species such as *G. bulloides*. As described previously, the
968 Mediterranean Sea has already been described as a climate change "hotspot", therefore the already
969 documented ocean warming and the consequent stratification (Malanotte-Rizzoli et al., 2014;
970 Siokou-Frangou et al., 2010) could have led to unfavorable conditions for several taxa. A decrease
971 in the primary production might have caused a shift in the dominance of the opportunistic *G.*
972 *bulloides* by *G. inflata*. As described previously, *G. bulloides* shows a high affinity for high
973 productivity environments, while deep dwellers such as *G. inflata* and *G. truncatulinoides* tend to
974 prefer mesotrophic and stratified waters. Finally, note that the high abundance of *G. bulloides* in
975 the seabed sediment could also be the result of a punctual high productivity events. In the Alboran
976 Sea, during upwelling events, big amounts of *G. bulloides* are deposited in the seabed and dominate
977 the assemblages, which reduces the relative abundance of other mesotrophic taxa (Bárcena et al.,
978 2004; Hernández-Almeida et al., 2011). Then, multiple recurring high productivity events occurring
979 over time in the Sicily Channel could explain the amount of *G. bulloides* in both the MARGO core-
980 tops and the sites 342 and 407. In that sense, the recent warming and stratification of the
981 Mediterranean could explain the recent trend in the planktonic foraminifera population registered
982 by the sediment trap. However, in that case, species such as *G. ruber* and other oligotrophic species
983 should be at least as much represented as in the seabed sediment. Alternatively, this could imply a
984 change in the intensity of the water masses flowing, such as an increased mesotrophic MAW
985 influence and a reduced oligotrophic LIW influence.
986 Additionally, from a chronological point of view, we propose that the main assemblage change
987 between the settling and the seabed sediment assemblages (i.e. the dominance of *G. inflata*) took
988 place during the late Holocene but preceded the industrial period. The Incarbona et al., (2019) dates
989 showed that, overall, since 1558 CE, *G. inflata* already dominated the samples. Also, the chronology
990 in the work from Margaritelli, (2020) coupled with the abundances presented in allowed to show
991 that, since the Little Ice Age, the three dominant species in the western Sicily Channel are *G. inflata*
992 followed by *G. ruber* and *G. bulloides*. This brings further confirmation that *G. inflata* dominated the
993 seabed sediment in the late Holocene, but also to the fact that the shift in the secondary species

994 (i.e. *G. truncatulinoides* instead of *G. ruber* and *G. bulloides*) is rather recent. Also, we assume that
995 the discrepancy with the MARGO core-tops sample is the result of the low temporal resolution.
996

997
998

999 **Figure 8.** Comparison of the relative abundance of the planktonic foraminifera from the sediment trap
1000 and seabed sediment. From top left to bottom right: the settling assemblage from the sediment is
1001 depicted in red; MARGO site 3655 corresponds to the lowest squared chord distance; the mean relative
1002 abundance of all MARGO sites included in this study (see Supplementary data); the results from the
1003 BONGO net retrieved in the Sicily Channel from Mallo et al., (2017); finally, the mean abundances (see
1004 section 3.5) from the two sites presented in Incarbona et al., (2019): sites 342 and 407.

1005

1006 **Table 3.** MARGO core-tops analyzed, their latitude and longitude and the squared chord distance (SCD)
1007 between the sediment trap in the C01 mooring line and the MARGO database core-tops. The complete
1008 SCD for all sites can be found in Supplementary data.

	MARGO database															
Site	3655	3677	3724	3739	3737	3738	3658	3725	3654	3680	3735	3736	3673	3727	3661	3726
Latitude	38.25	36.47	35.85	36.73	38.33	38.00	36.68	36.49	38.22	37.46	38.17	38.23	39.40	38.93	39.41	38.64
Longitude	13.35	11.49	13.03	13.95	11.80	11.78	12.28	13.32	13.27	11.55	11.23	11.25	13.34	10.59	13.34	10.78
SCD to C01	0.27	0.52	0.55	0.56	0.66	0.78	0.84	0.85	0.88	0.89	0.90	0.93	1.03	1.03	1.07	1.10

1009

1010   To document the differences between the assemblage in the C01 mooring line and the MARGO
1011   database core-tops, we hereby analyze the SCD between the annual integrated settling foraminifera
1012   assemblage of the C01 mooring line and all the core-tops located in the Sicily Channel (see
1013   Supplementary Figure 2). Overall, the SCD ranged between 0.27 and 1.1 (Table 3). By using a
1014   dissimilarity coefficient value of <0.25 as cutoff criteria (see section 3.6 for more details), it can be
1015   concluded that none of the core-tops assemblages can be considered close analogues to the C01
1016   mooring line. The only exception might be MARGO site 3655, located around 180 km northeast of
1017   the mooring line, which displayed an SCD value of 0.27, very close to our cutoff threshold.
1018   Interestingly, from a geographical point of view, the geographical closest site analyzed (MARGO
1019   3680) displayed a high SCD (0.89) despite being retrieved virtually in the underlying sediments
1020   beneath the C01 mooring line (Table 3). Overall, the 4 most similar sites (SCD <0.6) to the settling
1021   assemblage are all located eastward, while the 4 most different sites (SCD >1) are all located
1022   northward to the location of the mooring line. This highlights the geographical variability of the Sicily
1023   Channel regarding the planktonic foraminifera population and the complex oceanographic
1024   conditions. Note that, as mentioned previously, the lack of dating in these samples do not allow to
1025   bring further interpretations about the timing of planktonic foraminifera populations shifts. In
1026   addition to the lack of chronology control in these samples, no data is available for the
1027   sedimentation rate, which makes any assumption around the intensity of the hydrodynamics
1028   impossible. Finally, and as mentioned earlier, the retrieval method applied for the different core-
1029   tops could also be cited as source of the differences between the MARGO core-tops and with the
1030   sediment trap in the C01 mooring line. While a box-corer was used for sampling in sites 342 and 407
1031   (Incarbona et al., 2019), various devices were used for the MARGO core-tops, that includes piston
1032   and gravity cores that are known to often experience stretching or loss of material during the
1033   recovery of the sediments. Therefore, it is likely that the different MARGO surface sediment data
1034   set represent different time intervals.
1035   Taken into consideration all the uncertainties presented above, our data suggest that a change in
1036   the composition of the planktonic foraminifera assemblages took place at some stage of the late
1037   Holocene but before the onset of the industrial period. However, the available data precludes the
1038   determination of the main environmental drivers causing this change.
1039

1040   **Conclusions**

1041

1042   The C01 mooring line, located on the axis of the Sicily Channel, provided the opportunity to
1043   document the planktonic foraminifera population on an interannual scale. We analyzed 19 samples
1044   that covered the timespan between November 2013 and October 2014. A total of 3723 individuals
1045   and 15 different species were identified. *G. inflata*, *G. truncatulinoides*, *G. bulloides*, *G. ruber* and *G.*
1046   *ruber* (pink) were the five most abundant species, representing 56, 19, 8, 3.5 and 3% of the total
1047   foraminifera. The remaining species represented less than 5% of the total individuals. Total
1048   planktonic foraminifera flux ranged between 44 and 1890 shells $m^{-2} d^{-1}$, higher values were reached
1049   during spring while values were lower during summer. Our data indicates that the planktonic
1050   foraminifera fluxes mainly reflect the oceanographic configuration of the Sicily Channel and its
1051   seasonal surface circulation variability. During winter and spring, a stronger eastward advection

favours the MAW entrance in the Sicily Channel, allowing cool and nutrient enriched waters to enter the Channel. This resulted in an increased planktonic foraminifera flux and a higher presence of *G. inflata*, *G. truncatulinoides* or *G. bulloides*, which are taxa associated with the western basin. On the other hand, during summer, the eastward advection is reduced and the LIW dominates the water column, favorizing the increase of species associated with the eastern basin, such as *G. ruber*, and *G. ruber* (pink). Our correlation data with both SST and chlorophyll-*a* showed that *G. inflata* was associated with cool and nutrient rich waters. In contrast, both *G. ruber* species were associated with warm and oligotrophic waters, which agrees with their ecology. Surprisingly, no significant trends were identified for either *G. truncatulinoides* or *G. bulloides*. As *G. bulloides* flux increased coincidently with the benthic foraminifera one, we considered that this species might have a resuspended origin. The comparison with integrated annual data from other sediment trap experiments conducted in in different regions of the Mediterranean basin, our fluxes and diversity data indicated that the Sicily Channel can be considered a transitional zone in regard to planktonic foraminifera populations: annualized fluxes were lower compared to the westernmost Alboran Sea, but higher than in the easternmost Levantine basin. However, the Sicily Channel exhibited the highest diversity values across all the sites analyzed, highlighting the influence of both the western and eastern basins. Finally, the planktonic foraminifera assemblages from the sediment trap were also compared with seabed sediment assemblages. Overall, both eutrophic and oligotrophic taxa were more abundant in the seabed sediment, however, *G. inflata* dominated the assemblages in the closest samples to the sediment trap location. Our dataset was similar to the assemblages from sites 342 and 407 (Incarbona et al., 2019) but different than the ones from the MARGO core-tops. This is likely due to the fact that they represented different time periods. Finally, the high-resolution chronology from sites 342 and 407 allowed to show that the planktonic foraminifera population shift likely developed during the late Holocene prior to the industrial period. However, the causes of this shift remain uncertain, and our results call for increasing the monitoring of planktonic foraminifera populations and accentuating the comparisons between recent and seabed sediment assemblages in the Mediterranean to determine if the trends suggested by our data are the result of the recent environmental change.

1105

References

1107

1108 Aldridge, D., Beer, C. J., and Purdie, D. A.: Calcification in the planktonic foraminifera *Globigerina bulloides*; linked
1109   to phosphate concentrations in surface waters of the North Atlantic Ocean, Biogeosciences, 9, 1725–1739,
1110   https://doi.org/10.5194/bg-9-1725-2012, 2012.

1111 Álvarez, M., Sanleón-Bartolomé, H., Tanhua, T., Mintrop, L., Luchetta, A., Cantoni, C., Schroeder, K., and Civitarese,
1112   G.: The CO_2 system in the Mediterranean Sea: a basin wide perspective, Ocean Sci., 10, 69–92,
1113   https://doi.org/10.5194/os-10-69-2014, 2014.

1114 Astraldi, M., Gasparini, G. P., Gervasio, L., and Salusti, E.: Dense Water Dynamics along the Channel of Sicily
1115   (Mediterranean Sea), J. Phys. Oceanogr., 31, 3457–3475, https://doi.org/10.1175/1520-
1116   0485(2001)031<3457:DWDATS>2.0.CO;2, 2001.

1117 Astraldi, M., Gasparini, G. P., Vetrano, A., and Vignudelli, S.: Hydrographic characteristics and interannual
1118   variability of water masses in the central Mediterranean: a sensitivity test for long-term changes in the
1119   Mediterranean Sea, Deep Sea Research Part I: Oceanographic Research Papers, 49, 661–680,
1120   https://doi.org/10.1016/S0967-0637(01)00059-0, 2002.

1121 Avnaim-Katav, S., Herut, B., Rahav, E., Katz, T., Weinstein, Y., Alkalay, R., Berman-Frank, I., Zlatkin, O., and Almogi-
1122   Labin, A.: Sediment trap and deep sea coretop sediments as tracers of recent changes in planktonic
1123   foraminifera assemblages in the southeastern ultra-oligotrophic Levantine Basin, Deep Sea Research Part II:
1124   Topical Studies in Oceanography, 171, 104669, https://doi.org/10.1016/j.dsr2.2019.104669, 2020.

1125 Azibeiro, L. A., Kučera, M., Jonkers, L., Cloke-Hayes, A., and Sierro, F. J.: Nutrients and hydrography explain the
1126   composition of recent Mediterranean planktonic foraminiferal assemblages, Marine Micropaleontology, 179,
1127   102201, https://doi.org/10.1016/j.marmicro.2022.102201, 2023.

1128 Balestra, B., Grunert, P., Ausin, B., Hodell, D., Flores, J.-A., Alvarez-Zarikian, C. A., Hernandez-Molina, F. J., Stow, D.,
1129   Piller, W. E., and Paytan, A.: Coccolithophore and benthic foraminifera distribution patterns in the Gulf of
1130   Cadiz and Western Iberian Margin during Integrated Ocean Drilling Program (IODP) Expedition 339, Journal of
1131   Marine Systems, 170, 50–67, https://doi.org/10.1016/j.jmarsys.2017.01.005, 2017.

1132 Bárcena, M. A., Flores, J. A., Sierro, F. J., Pérez-Folgado, M., Fabres, J., Calafat, A., and Canals, M.: Planktonic
1133   response to main oceanographic changes in the Alboran Sea (Western Mediterranean) as documented in
1134   sediment traps and surface sediments, Marine Micropaleontology, 53, 423–445,
1135   https://doi.org/10.1016/j.marmicro.2004.09.009, 2004.

1136 Barker, S. and Elderfield, H.: Foraminiferal Calcification Response to Glacial-Interglacial Changes in Atmospheric
1137 CO_2, Science, 297, 833–836, https://doi.org/10.1126/science.1072815, 2002.

1138 Bé, A. W. H., Hutson, W. H., and Be, A. W. H.: Ecology of Planktonic Foraminifera and Biogeographic Patterns of
1139   Life and Fossil Assemblages in the Indian Ocean, Micropaleontology, 23, 369,
1140   https://doi.org/10.2307/1485406, 1977.

1141 Beer, C. J., Schiebel, R., and Wilson, P. A.: Testing planktonic foraminiferal shell weight as a surface water [CO32−]
1142   proxy using plankton net samples, Geology, 38, 103–106, https://doi.org/10.1130/G30150.1, 2010.

Béjard, T. M., Rigual-Hernández, A. S., Flores, J. A., Tarruella, J. P., Durrieu De Madron, X., Cacho, I., Haghipour, N., Hunter, A., and Sierro, F. J.: Calcification response of planktonic foraminifera to environmental change in the western Mediterranean Sea during the industrial era, Biogeosciences, 20, 1505–1528, https://doi.org/10.5194/bg-20-1505-2023, 2023.

Béranger, K., Mortier, L., Gasparini, G.-P., Gervasio, L., Astraldi, M., and Crépon, M.: The dynamics of the Sicily Channel: a comprehensive study from observations and models, Deep Sea Research Part II: Topical Studies in Oceanography, 51, 411–440, https://doi.org/10.1016/j.dsr2.2003.08.004, 2004.

Bergamasco, A. and Malanotte-Rizzoli, P.: The circulation of the Mediterranean Sea: a historical review of experimental investigations, Advances in Oceanography and Limnology, 1, 11–28, https://doi.org/10.1080/19475721.2010.491656, 2010.

Bethoux, J. P., Gentili, B., Morin, P., Nicolas, E., Pierre, C., and Ruiz-Pino, D.: The Mediterranean Sea: a miniature ocean for climatic and environmental studies and a key for the climatic functioning of the North Atlantic, Progress in Oceanography, 44, 131–146, https://doi.org/10.1016/S0079-6611(99)00023-3, 1999.

Bijma, J., Faber, W. W., and Hemleben, C.: Temperature and salinity limits for growth and survival of some planktonic foraminifers in laboratory cultures, The Journal of Foraminiferal Research, 20, 95–116, https://doi.org/10.2113/gsjfr.20.2.95, 1990.

Bijma, J., Hönisch, B., and Zeebe, R. E.: Impact of the ocean carbonate chemistry on living foraminiferal shell weight: Comment on "Carbonate ion concentration in glacial-age deep waters of the Caribbean Sea" by W. S. Broecker and E. Clark: COMMENT, Geochem.-Geophys.-Geosyst., 3, 1–7, https://doi.org/10.1029/2002GC000388, 2002.

Bouzinac, C., Font, J., and Millot, C.: Hydrology and currents observed in the channel of Sardinia during the PRIMO-1 experiment from November 1993 to October 1994, Journal of Marine Systems, 20, 333–355, https://doi.org/10.1016/S0924-7963(98)00074-8, 1999.

Chapman, M. R.: Seasonal production patterns of planktonic foraminifera in the NE Atlantic Ocean: Implications for paleotemperature and hydrographic reconstructions: CURRENTS, Paleoceanography, 25, https://doi.org/10.1029/2008PA001708, 2010.

Chernihovsky, N., Torfstein, A., and Almogi-Labin, A.: Seasonal flux patterns of planktonic foraminifera in a deep, oligotrophic, marginal sea: Sediment trap time series from the Gulf of Aqaba, northern Red Sea, Deep Sea Research Part I: Oceanographic Research Papers, 140, 78–94, https://doi.org/10.1016/j.dsr.2018.08.003, 2018.

Chernihovsky, N., Torfstein, A., and Almogi-Labin, A.: Daily timescale dynamics of planktonic foraminifera shell-size distributions, Front. Mar. Sci., 10, 1126398, https://doi.org/10.3389/fmars.2023.1126398, 2023.

Cisneros, M., Cacho, I., Frigola, J., Canals, M., Masqué, P., Martrat, B., Casado, M., Grimalt, J. O., Pena, L. D., Margaritelli, G., and Lirer, F.: Sea surface temperature variability in the central-western Mediterranean Sea during the last 2700 years: a multi-proxy and multi-record approach, Clim. Past, 12, 849–869, https://doi.org/10.5194/cp-12-849-2016, 2016.

Dittert, N., Baumann, K.-H., Bickert, T., Henrich, R., Huber, R., Kinkel, H., and Meggers, H.: Carbonate Dissolution in the Deep-Sea: Methods, Quantification and Paleoceanographic Application, in: Use of Proxies in Paleoceanography, edited by: Fischer, G. and Wefer, G., Springer Berlin Heidelberg, Berlin, Heidelberg, 255–284, https://doi.org/10.1007/978-3-642-58646-0_10, 1999.

D'Ortenzio, F.: On the trophic regimes of the Mediterranean Sea: a satellite analysis, 2009.

Ducassou, E., Hassan, R., Gonthier, E., Duprat, J., Hanquiez, V., and Mulder, T.: Biostratigraphy of the last 50 kyr in the contourite depositional system of the Gulf of Cádiz, Marine Geology, 395, 285–300, https://doi.org/10.1016/j.margeo.2017.09.014, 2018.

Durrieu de Madron, X., Houpert, L., Puig, P., Sanchez-Vidal, A., Testor, P., Bosse, A., Estournel, C., Somot, S., Bourrin, F., Bouin, M. N., Beauverger, M., Beguery, L., Calafat, A., Canals, M., Cassou, C., Coppola, L., Dausse, D., D'Ortenzio, F., Font, J., Heussner, S., Kunesch, S., Lefevre, D., Le Goff, H., Martín, J., Mortier, L., Palanques, A., and Raimbault, P.: Interaction of dense shelf water cascading and open-sea convection in the northwestern Mediterranean during winter 2012: SHELF CASCADING AND OPEN-SEA CONVECTION, Geophys. Res. Lett., 40, 1379–1385, https://doi.org/10.1002/grl.50331, 2013.

Fox, L., Stukins, S., Hill, T., and Miller, C. G.: Quantifying the Effect of Anthropogenic Climate Change on Calcifying Plankton, Sci Rep, 10, 1620, https://doi.org/10.1038/s41598-020-58501-w, 2020.

Garcia-Solsona, E., Pena, L. D., Paredes, E., Pérez-Asensio, J. N., Quirós-Collazos, L., Lirer, F., and Cacho, I.: Rare earth elements and Nd isotopes as tracers of modern ocean circulation in the central Mediterranean Sea, Progress in Oceanography, 185, 102340, https://doi.org/10.1016/j.pocean.2020.102340, 2020.

Gasparini, G. P., Smeed, D. A., Alderson, S., Sparnocchia, S., Vetrano, A., and Mazzola, S.: Tidal and subtidal currents in the Strait of Sicily, J. Geophys. Res., 109, 2003JC002011, https://doi.org/10.1029/2003JC002011, 2004.

Gasparini, G. P., Ortona, A., Budillon, G., Astraldi, M., and Sansone, E.: The effect of the Eastern Mediterranean Transient on the hydrographic characteristics in the Channel of Sicily and in the Tyrrhenian Sea, Deep Sea Research Part I: Oceanographic Research Papers, 52, 915–935, https://doi.org/10.1016/j.dsr.2005.01.001, 2005.

Gaudy, R., Youssara, F., Diaz, F., and Raimbault, P.: Biomass, metabolism and nutrition of zooplankton in the Gulf of Lions (NW Mediterranean), Oceanologica Acta, 26, 357–372, https://doi.org/10.1016/S0399-1784(03)00016-1, 2003.

Grifoll, M., Cerralbo, P., Guillén, J., Espino, M., Hansen, L. B., and Sánchez-Arcilla, A.: Characterization of bottom sediment resuspension events observed in a micro-tidal bay, Ocean Sci., 15, 307–319, https://doi.org/10.5194/os-15-307-2019, 2019.

Hassoun, A. E. R., Gemayel, E., Krasakopoulou, E., Goyet, C., Abboud-Abi Saab, M., Guglielmi, V., Touratier, F., and Falco, C.: Acidification of the Mediterranean Sea from anthropogenic carbon penetration, Deep Sea Research Part I: Oceanographic Research Papers, 102, 1–15, https://doi.org/10.1016/j.dsr.2015.04.005, 2015.

Hassoun, A. E. R., Bantelman, A., Canu, D., Comeau, S., Galdies, C., Gattuso, J.-P., Giani, M., Grelaud, M., Hendriks, I. E., Ibello, V., Idrissi, M., Krasakopoulou, E., Shaltout, N., Solidoro, C., Swarzenski, P. W., and Ziveri, P.: Ocean acidification research in the Mediterranean Sea: Status, trends and next steps, Front. Mar. Sci., 9, 892670, https://doi.org/10.3389/fmars.2022.892670, 2022.

Hayes, A., Kucera, M., Kallel, N., Sbaffi, L., and Rohling, E. J.: Compilation of planktonic foraminifera modern data from the Mediterranean Sea, https://doi.org/10.1594/PANGAEA.227305, 2005.

Hazan, O., Silverman, J., Sisma-Ventura, G., Ozer, T., Gertman, I., Shoham-Frider, E., Kress, N., and Rahav, E.: Mesopelagic Prokaryotes Alter Surface Phytoplankton Production during Simulated Deep Mixing Experiments in Eastern Mediterranean Sea Waters, Front. Mar. Sci., 5, 1, https://doi.org/10.3389/fmars.2018.00001, 2018.

Hemleben, C., Spindler, M., and Anderson, O. R.: Modern Planktonic Foraminifera, 1989.

Hernández-Almeida, I., Bárcena, M. A., Flores, J. A., Sierro, F. J., Sanchez-Vidal, A., and Calafat, A.: Microplankton response to environmental conditions in the Alboran Sea (Western Mediterranean): One year sediment trap record, Marine Micropaleontology, 78, 14–24, https://doi.org/10.1016/j.marmicro.2010.09.005, 2011.

Heussner, S., Ratti, C., and Carbonne, J.: The PPS 3 time-series sediment trap and the trap sample processing techniques used during the ECOMARGE experiment, Continental Shelf Research, 10, 943–958, https://doi.org/10.1016/0278-4343(90)90069-X, 1990.

Heussner, S., Durrieu de Madron, X., Calafat, A., Canals, M., Carbonne, J., Delsaut, N., and Saragoni, G.: Spatial and temporal variability of downward particle fluxes on a continental slope: Lessons from an 8-yr experiment in the Gulf of Lions (NW Mediterranean), Marine Geology, 234, 63–92, https://doi.org/10.1016/j.margeo.2006.09.003, 2006.

Houpert, L., Durrieu de Madron, X., Testor, P., Bosse, A., D'Ortenzio, F., Bouin, M. N., Dausse, D., Le Goff, H., Kunesch, S., Labaste, M., Coppola, L., Mortier, L., and Raimbault, P.: Observations of open-ocean deep convection in the northwestern Mediterranean Sea: Seasonal and interannual variability of mixing and deep water masses for the 2007-2013 Period: DEEP CONVECTION OBS. NWMED 2007-2013, J. Geophys. Res. Oceans, 121, 8139–8171, https://doi.org/10.1002/2016JC011857, 2016.

Huertas, I. E., Ríos, A. F., García-Lafuente, J., Navarro, G., Makaoui, A., Sánchez-Román, A., Rodriguez-Galvez, S., Orbi, A., Ruíz, J., and Pérez, F. F.: Atlantic forcing of the Mediterranean oligotrophy: ATLANTIC FORCING OF MEDITERRANEAN OLIGOTROPHY, Global Biogeochem. Cycles, 26, n/a-n/a, https://doi.org/10.1029/2011GB004167, 2012.

Incarbona, A., Jonkers, L., Ferraro, S., Sprovieri, R., and Tranchida, G.: Sea Surface Temperatures and Paleoenvironmental Variability in the Central Mediterranean During Historical Times Reconstructed Using Planktonic Foraminifera, Paleoceanog and Paleoclimatol, 34, 394–408, https://doi.org/10.1029/2018PA003529, 2019.

Incarbona, A., Sprovieri, M., Lirer, F., and Sprovieri, R.: Surface and deep water conditions in the Sicily channel (central Mediterranean) at the time of sapropel S5 deposition, Palaeogeography, Palaeoclimatology, Palaeoecology, 306, 243–248, https://doi.org/10.1016/j.palaeo.2011.04.030, 2011.

Jonkers, L. and Kučera, M.: Global analysis of seasonality in the shell flux of extant planktonic Foraminifera, Biogeosciences, 12, 2207–2226, https://doi.org/10.5194/bg-12-2207-2015, 2015.

Jonkers, L., Hillebrand, H., and Kucera, M.: Global change drives modern plankton communities away from the pre-industrial state, Nature, 570, 372–375, https://doi.org/10.1038/s41586-019-1230-3, 2019.

Jouini, M., Béranger, K., Arsouze, T., Beuvier, J., Thiria, S., Crépon, M., and Taupier-Letage, I.: The Sicily Channel surface circulation revisited using a neural clustering analysis of a high-resolution simulation, JGR Oceans, 121, 4545–4567, https://doi.org/10.1002/2015JC011472, 2016.

Kemle-von Mücke, S. and Oberhänsli, H.: The Distribution of Living Planktonic Foraminifera in Relation to Southeast Atlantic Oceanography, in: Use of Proxies in Paleoceanography, edited by: Fischer, G. and Wefer, G., Springer Berlin Heidelberg, Berlin, Heidelberg, 91–115, https://doi.org/10.1007/978-3-642-58646-0_3, 1999.

Kiss, P., Jonkers, L., Hudáčková, N., Reuter, R. T., Donner, B., Fischer, G., and Kucera, M.: Determinants of Planktonic Foraminifera Calcite Flux: Implications for the Prediction of Intra- and Inter-Annual Pelagic Carbonate Budgets, Global Biogeochem Cycles, 35, https://doi.org/10.1029/2020GB006748, 2021.

Kroeker, K. J., Kordas, R. L., Crim, R., Hendriks, I. E., Ramajo, L., Singh, G. S., Duarte, C. M., and Gattuso, J.: Impacts of ocean acidification on marine organisms: quantifying sensitivities and interaction with warming, Glob Change Biol, 19, 1884–1896, https://doi.org/10.1111/gcb.12179, 2013.

Krom, M. D., Kress, N., Brenner, S., and Gordon, L. I.: Phosphorus limitation of primary productivity in the eastern Mediterranean Sea, Limnol. Oceanogr., 36, 424–432, https://doi.org/10.4319/lo.1991.36.3.0424, 1991.

Krom, M. D., Woodward, E. M. S., Herut, B., Kress, N., Carbo, P., Mantoura, R. F. C., Spyres, G., Thingstad, T. F., Wassmann, P., Wexels-Riser, C., Kitidis, V., Law, C. S., and Zodiatis, G.: Nutrient cycling in the south east Levantine basin of the eastern Mediterranean: Results from a phosphorus starved system, Deep Sea Research Part II: Topical Studies in Oceanography, 52, 2879–2896, https://doi.org/10.1016/j.dsr2.2005.08.009, 2005.

Kuroyanagi, A. and Kawahata, H.: Vertical distribution of living planktonic foraminifera in the seas around Japan, Marine Micropaleontology, 53, 173–196, https://doi.org/10.1016/j.marmicro.2004.06.001, 2004.

Lazzari, P., Mattia, G., Solidoro, C., Salon, S., Crise, A., Zavatarelli, M., Oddo, P., and Vichi, M.: The impacts of climate change and environmental management policies on the trophic regimes in the Mediterranean Sea: Scenario analyses, Journal of Marine Systems, 135, 137–149, https://doi.org/10.1016/j.jmarsys.2013.06.005, 2014.

Lermusiaux, P. F. J. and Robinson, A. R.: Features of dominant mesoscale variability, circulation patterns and dynamics in the Channel of Sicily, Deep Sea Research Part I: Oceanographic Research Papers, 48, 1953–1997, https://doi.org/10.1016/S0967-0637(00)00114-X, 2001.

Lirer, F., Sprovieri, M., Vallefuoco, M., Ferraro, L., Pelosi, N., Giordano, L., and Capotondi, L.: Planktonic foraminifera as bio-indicators for monitoring the climatic changes that have occurred over the past 2000 years in the southeastern Tyrrhenian Sea, Integrative Zoology, 9, 542–554, https://doi.org/10.1111/1749-4877.12083, 2014.

Lombard, F., Erez, J., Michel, E., and Labeyrie, L.: Temperature effect on respiration and photosynthesis of the symbiont-bearing planktonic foraminifera *Globigerinoides ruber* , *Orbulina universa* , and *Globigerinella siphonifera*, Limnol. Oceanogr., 54, 210–218, https://doi.org/10.4319/lo.2009.54.1.0210, 2009.

Lombard, F., Labeyrie, L., Michel, E., Bopp, L., Cortijo, E., Retailleau, S., Howa, H., and Jorissen, F.: Modelling planktonic foraminifer growth and distribution using an ecophysiological multi-species approach, Biogeosciences, 8, 853–873, https://doi.org/10.5194/bg-8-853-2011, 2011.

Macias, D., Cózar, A., Garcia-Gorriz, E., González-Fernández, D., and Stips, A.: Surface water circulation develops seasonally changing patterns of floating litter accumulation in the Mediterranean Sea. A modelling approach, Marine Pollution Bulletin, 149, 110619, https://doi.org/10.1016/j.marpolbul.2019.110619, 2019.

Malanotte-Rizzoli, P., Artale, V., Borzelli-Eusebi, G. L., Brenner, S., Crise, A., Gacic, M., Kress, N., Marullo, S., Ribera d'Alcalà, M., Sofianos, S., Tanhua, T., Theocharis, A., Alvarez, M., Ashkenazy, Y., Bergamasco, A., Cardin, V., Carniel, S., Civitarese, G., D'Ortenzio, F., Font, J., Garcia-Ladona, E., Garcia-Lafuente, J. M., Gogou, A., Gregoire, M., Hainbucher, D., Kontoyannis, H., Kovacevic, V., Kraskapoulou, E., Kroskos, G., Incarbona, A., Mazzocchi, M. G., Orlic, M., Ozsoy, E., Pascual, A., Poulain, P.-M., Roether, W., Rubino, A., Schroeder, K., Siokou-Frangou, J., Souvermezoglou, E., Sprovieri, M., Tintoré, J., and Triantafyllou, G.: Physical forcing and

1299   physical/biochemical variability of the Mediterranean Sea: a review of unresolved issues and directions for
1300   future research, Ocean Sci., 10, 281–322, https://doi.org/10.5194/os-10-281-2014, 2014.

1301 Mallo, M., Ziveri, P., Mortyn, P. G., Schiebel, R., and Grelaud, M.: Low planktonic foraminiferal diversity and
1302   abundance observed in a spring 2013 west–east Mediterranean Sea plankton tow transect, Biogeosciences,
1303   14, 2245–2266, https://doi.org/10.5194/bg-14-2245-2017, 2017.

1304 Margaritelli, G., Lirer, F., Schroeder, K., Alberico, I., Dentici, M. P., and Caruso, A.: Globorotalia truncatulinoides in
1305   Central - Western Mediterranean Sea during the Little Ice Age, Marine Micropaleontology, 161, 101921,
1306   https://doi.org/10.1016/j.marmicro.2020.101921, 2020.

1307 Margaritelli, G., Lirer, F., Schroeder, K., Cloke-Hayes, A., Caruso, A., Capotondi, L., Broggy, T., Cacho, I., and Sierro,
1308   F. J.: Globorotalia truncatulinoides in the Mediterranean Basin during the Middle–Late Holocene: Bio-
1309   Chronological and Oceanographic Indicator, Geosciences, 12, 244,
1310   https://doi.org/10.3390/geosciences12060244, 2022.

1311 Marshall, B. J., Thunell, R. C., Henehan, M. J., Astor, Y., and Wejnert, K. E.: Planktonic foraminiferal area density as
1312   a proxy for carbonate ion concentration: A calibration study using the Cariaco Basin ocean time series:
1313   FORAMINIFERAL AREA DENSITY [CO_3^{2-}] PROXY, Paleoceanography, 28, 363–376,
1314   https://doi.org/10.1002/palo.20034, 2013.

1315 Milker, Y. and Schmiedl, G.: A taxonomic guide to modern benthic shelf foraminifera of the western Mediterranean
1316   Sea, Palaeontologia Electronica, https://doi.org/10.26879/271, 2012.

1317 Millot, C.: Mesoscale and seasonal variabilities of the circulation in the western Mediterranean, Dynamics of
1318   Atmospheres and Oceans, 15, 179–214, https://doi.org/10.1016/0377-0265(91)90020-G, 1991.

1319 Millot, C.: Circulation in the Western Mediterranean Sea, Journal of Marine Systems, 20, 423–442,
1320   https://doi.org/10.1016/S0924-7963(98)00078-5, 1999.

1321 Millot, C. and Taupier-Letage, I.: Circulation in the Mediterranean Sea, in: The Mediterranean Sea, vol. 5K, edited
1322   by: Saliot, A., Springer Berlin Heidelberg, Berlin, Heidelberg, 29–66, https://doi.org/10.1007/b107143, 2005.

1323 de Moel, H., Ganssen, G. M., Peeters, F. J. C., Jung, S. J. A., Kroon, D., Brummer, G. J. A., and Zeebe, R. E.: Planktonic
1324   foraminiferal shell thinning in the Arabian Sea due to anthropogenic ocean acidification?, Biogeosciences, 6,
1325   1917–1925, https://doi.org/10.5194/bg-6-1917-2009, 2009.

1326 Morán, X. and Estrada, M.: Short-term variability of photosynthetic parameters and particulate and dissolved
1327   primary production in the Alboran Sea (SW Mediterranean), Mar. Ecol. Prog. Ser., 212, 53–67,
1328   https://doi.org/10.3354/meps212053, 2001.

1329 Moy, A. D., Howard, W. R., Bray, S. G., and Trull, T. W.: Reduced calcification in modern Southern Ocean planktonic
1330   foraminifera, Nature Geosci, 2, 276–280, https://doi.org/10.1038/ngeo460, 2009.

1331 Navarro, G., Almaraz, P., Caballero, I., Vázquez, Á., and Huertas, I. E.: Reproduction of Spatio-Temporal Patterns of
1332   Major Mediterranean Phytoplankton Groups from Remote Sensing OC-CCI Data, Front. Mar. Sci., 4, 246,
1333   https://doi.org/10.3389/fmars.2017.00246, 2017.

1334 Nielsen, S. N.: Numerical Ecology. Legendre P. and Legendre L., second ed., Elsevier, Amsterdam, p. 853, 1998.,
1335   Ecological Modelling, 132, 303–304, https://doi.org/10.1016/S0304-3800(00)00291-X, 2000.

1336 Ortiz, J. D. and Mix, A. C.: Comparison of Imbrie-Kipp Transfer Function and modern analog temperature estimates
1337   using sediment trap and core top foraminiferal faunas, Paleoceanography, 12, 175–190,
1338   https://doi.org/10.1029/96PA02878, 1997.

1339 Osborne, E. B., Thunell, R. C., Marshall, B. J., Holm, J. A., Tappa, E. J., Benitez-Nelson, C., Cai, W., and Chen, B.:
1340   Calcification of the planktonic foraminifera *Globigerina bulloides* and carbonate ion concentration: Results
1341   from the Santa Barbara Basin, Paleoceanography, 31, 1083–1102, https://doi.org/10.1002/2016PA002933,
1342   2016.

1343 Ozer, T., Gertman, I., Kress, N., Silverman, J., and Herut, B.: Interannual thermohaline (1979–2014) and nutrient
1344   (2002–2014) dynamics in the Levantine surface and intermediate water masses, SE Mediterranean Sea, Global
1345   and Planetary Change, 151, 60–67, https://doi.org/10.1016/j.gloplacha.2016.04.001, 2017.

1346 Pallacks, S., Ziveri, P., Schiebel, R., Vonhof, H., Rae, J. W. B., Littley, E., Garcia-Orellana, J., Langer, G., Grelaud, M.,
1347   and Martrat, B.: Anthropogenic acidification of surface waters drives decreased biogenic calcification in the
1348   Mediterranean Sea, Commun Earth Environ, 4, 301, https://doi.org/10.1038/s43247-023-00947-7, 2023.

1349 Pinardi, N., Zavatarelli, M., Adani, M., Coppini, G., Fratianni, C., Oddo, P., Simoncelli, S., Tonani, M., Lyubartsev, V.,
1350   Dobricic, S., and Bonaduce, A.: Mediterranean Sea large-scale low-frequency ocean variability and water mass

1351   formation rates from 1987 to 2007: A retrospective analysis, Progress in Oceanography, 132, 318–332,
1352   https://doi.org/10.1016/j.pocean.2013.11.003, 2015.

1353 Poore, R. Z., Tedesco, K. A., and Spear, J. W.: Seasonal Flux and Assemblage Composition of Planktonic Foraminifers
1354   from a Sediment-Trap Study in the Northern Gulf of Mexico, Journal of Coastal Research, 63, 6–19,
1355   https://doi.org/10.2112/SI63-002.1, 2013.

1356 Prell, W. The Stability of Low-Latitude Sea-Surface Temperatures, an Evaluation of the CLIMAP Reconstruction with
1357   Emphasis on the Positive SST Anomalies. *Report No. TR025* (US Department of Energy), 1985.

1358 Pujol, C. and Grazzini, C. V.: Distribution patterns of live planktonic foraminifers as related to regional hydrography
1359   and productive systems of the Mediterranean Sea, Marine Micropaleontology, 25, 187–217,
1360   https://doi.org/10.1016/0377-8398(95)00002-I, 1995.

1361 Raimbault, P., Pouvesle, W., Diaz, F., Garcia, N., and Sempéré, R.: Wet-oxidation and automated colorimetry for
1362   simultaneous determination of organic carbon, nitrogen and phosphorus dissolved in seawater, Marine
1363   Chemistry, 66, 161–169, https://doi.org/10.1016/S0304-4203(99)00038-9, 1999.

1364 Rebotim, A., Voelker, A. H. L., Jonkers, L., Waniek, J. J., Meggers, H., Schiebel, R., Fraile, I., Schulz, M., and Kucera,
1365   M.: Factors controlling the depth habitat of planktonic foraminifera in the subtropical eastern North Atlantic,
1366   Biogeosciences, 14, 827–859, https://doi.org/10.5194/bg-14-827-2017, 2017.

1367 Retailleau, S., Schiebel, R., and Howa, H.: Population dynamics of living planktonic foraminifers in the hemipelagic
1368   southeastern Bay of Biscay, Marine Micropaleontology, 80, 89–100,
1369   https://doi.org/10.1016/j.marmicro.2011.06.003, 2011.

1370 Rigual-Hernández, A. S., Sierro, F. J., Bárcena, M. A., Flores, J. A., and Heussner, S.: Seasonal and interannual
1371   changes of planktonic foraminiferal fluxes in the Gulf of Lions (NW Mediterranean) and their implications for
1372   paleoceanographic studies: Two 12-year sediment trap records, Deep Sea Research Part I: Oceanographic
1373   Research Papers, 66, 26–40, https://doi.org/10.1016/j.dsr.2012.03.011, 2012.

1374 Robinson, A. R. and Golnaraghi, M.: The Physical and Dynamical Oceanography of the Mediterranean Sea, in:
1375   Ocean Processes in Climate Dynamics: Global and Mediterranean Examples, edited by: Malanotte-Rizzoli, P.
1376   and Robinson, A. R., Springer Netherlands, Dordrecht, 255–306, https://doi.org/10.1007/978-94-011-0870-
1377   6_12, 1994.

1378 Robinson, A. R., Sellschopp, J., Warn-Varnas, A., Leslie, W. G., Lozano, C. J., Haley Jr, P. J., Anderson, L. A., and
1379   Lermusiaux, P. F. J.: The Atlantic Ionian Stream, Journal of Marine Systems, 129–156, 1999.

1380 Romero, O., Boeckel, B., Donner, B., Lavik, G., Fischer, G., and Wefer, G.: Seasonal productivity dynamics in the
1381   pelagic central Benguela System inferred from the flux of carbonate and silicate organisms, Journal of Marine
1382   Systems, 37, 259–278, https://doi.org/10.1016/S0924-7963(02)00189-6, 2002.

1383 Salmon, K. H., Anand, P., Sexton, P. F., and Conte, M.: Upper ocean mixing controls the seasonality of planktonic
1384   foraminifer fluxes and associated strength of the carbonate pump in the oligotrophic North Atlantic,
1385   Biogeosciences, 12, 223–235, https://doi.org/10.5194/bg-12-223-2015, 2015.

1386 Schiebel, R.: Planktonic foraminiferal sedimentation and the marine calcite budget: MARINE CALCITE BUDGET,
1387   Global Biogeochem. Cycles, 16, 3-1-3–21, https://doi.org/10.1029/2001GB001459, 2002.

1388 Schiebel, R. and Hemleben, C.: Modern planktonic foraminifera, Paläontol. Z., 79, 135–148,
1389   https://doi.org/10.1007/BF03021758, 2005.

1390 Schiebel, R. and Hemleben, C.: Planktonic Foraminifers in the Modern Ocean, Springer Berlin Heidelberg, Berlin,
1391   Heidelberg, https://doi.org/10.1007/978-3-662-50297-6, 2017.

1392 Schiebel, R., Waniek, J., Bork, M., and Hemleben, C.: Planktonic foraminiferal production stimulated by chlorophyll
1393   redistribution and entrainment of nutrients, Deep Sea Research Part I: Oceanographic Research Papers, 48,
1394   721–740, https://doi.org/10.1016/S0967-0637(00)00065-0, 2001.

1395 Schiebel, R., Zeltner, A., Treppke, U. F., Waniek, J. J., Bollmann, J., Rixen, T., and Hemleben, C.: Distribution of
1396   diatoms, coccolithophores and planktonic foraminifers along a trophic gradient during SW monsoon in the
1397   Arabian Sea, Marine Micropaleontology, 51, 345–371, https://doi.org/10.1016/j.marmicro.2004.02.001,
1398   2004.

1399 Schmidt, D. N., Lazarus, D., Young, J. R., and Kucera, M.: Biogeography and evolution of body size in marine
1400   plankton, Earth-Science Reviews, 78, 239–266, https://doi.org/10.1016/j.earscirev.2006.05.004, 2006.

1401 Schroeder, K., Chiggiato, J., Josey, S. A., Borghini, M., Aracri, S., and Sparnocchia, S.: Rapid response to climate
1402   change in a marginal sea, Sci Rep, 7, 4065, https://doi.org/10.1038/s41598-017-04455-5, 2017.

1403 Schroeder, K., Gasparini, G. P., Borghini, M., Cerrati, G., and Delfanti, R.: Biogeochemical tracers and fluxes in the
1404   Western Mediterranean Sea, spring 2005, Journal of Marine Systems, 80, 8–24,
1405   https://doi.org/10.1016/j.jmarsys.2009.08.002, 2010.
1406 Sen Gupta, B. K. (Ed.): Modern foraminifera, first published in paperback., Kluwer, Dordrecht, 371 pp., 2002.
1407 Siccha, M. and Kucera, M.: ForCenS, a curated database of planktonic foraminifera census counts in marine surface
1408   sediment samples, Sci Data, 4, 170109, https://doi.org/10.1038/sdata.2017.109, 2017.
1409 Siokou-Frangou, I., Christaki, U., Mazzocchi, M. G., Montresor, M., Ribera d'Alcalá, M., Vaqué, D., and Zingone, A.:
1410   Plankton in the open Mediterranean Sea: a review, Biogeosciences, 7, 1543–1586,
1411   https://doi.org/10.5194/bg-7-1543-2010, 2010.
1412 Skinner, L. C. and McCave, I. N.: Analysis and modelling of gravity- and piston coring based on soil mechanics,
1413   Marine Geology, 199, 181–204, https://doi.org/10.1016/S0025-3227(03)00127-0, 2003.
1414 Takagi, H., Kimoto, K., Fujiki, T., Saito, H., Schmidt, C., Kucera, M., and Moriya, K.: Characterizing photosymbiosis
1415   in modern planktonic foraminifera, Biogeosciences, 16, 3377–3396, https://doi.org/10.5194/bg-16-3377-
1416   2019, 2019.
1417 Takahashi, K. and Be, A. W. H.: Planktonic foraminifera: factors controlling sinking speeds, Deep Sea Research Part
1418   A. Oceanographic Research Papers, 31, 1477–1500, https://doi.org/10.1016/0198-0149(84)90083-9, 1984.
1419 Toucanne, S., Mulder, T., Schönfeld, J., Hanquiez, V., Gonthier, E., Duprat, J., Cremer, M., and Zaragosi, S.:
1420   Contourites of the Gulf of Cadiz: A high-resolution record of the paleocirculation of the Mediterranean outflow
1421   water during the last 50,000 years, Palaeogeography, Palaeoclimatology, Palaeoecology, 246, 354–366,
1422   https://doi.org/10.1016/j.palaeo.2006.10.007, 2007.
1423 Warn-Varnas, A., Sellschopp, J., Haley, P. J., Leslie, W. G., and Lozano, C. J.: Channel of Sicily water masses,
1424   Dynamics of Atmospheres and Oceans, 29, 437–469, https://doi.org/10.1016/S0377-0265(99)00014-7, 1999.
1425 Wilke, I., Meggers, H., and Bickert, T.: Depth habitats and seasonal distributions of recent planktonic foraminifers
1426   in the Canary Islands region (29°N) based on oxygen isotopes, Deep Sea Research Part I: Oceanographic
1427   Research Papers, 56, 89–106, https://doi.org/10.1016/j.dsr.2008.08.001, 2009.
1428 Wu, H., Liu, N., Peng, J., Ge, Y., and Kong, B.: Analysis and modelling on coring process of deep-sea gravity piston
1429   corer, J. eng., 2020, 900–905, https://doi.org/10.1049/joe.2020.0077, 2020.
1430 Wolfteich, C. M.: Sattelite-derived sea surface temperature, mesoscale variability, and foraminiferal production in
1431   the North Atlantic, M.Sc., MIT and WHOI, Cambridge, MS, 91 pp., 1994.
1432 Zarkogiannis, S. D., Iwasaki, S., Rae, J. W. B., Schmidt, M. W., Mortyn, P. G., Kontakiotis, G., Hertzberg, J. E., and
1433   Rickaby, R. E. M.: Calcification, Dissolution and Test Properties of Modern Planktonic Foraminifera From the
1434   Central Atlantic Ocean, Front. Mar. Sci., 9, 864801, https://doi.org/10.3389/fmars.2022.864801, 2022.
1435
1436
1437
1438
1439